Food Safety) from the Ministry of Health, Labor and Welfare of Japan.

References

1) Bhat, R.V., Beedu, S.R., Ramakrishna, Y., Munshi, K.L.: Lancet, **1**, 35-37 (1989)
2) Abbas, H.K, Mirocha, C.J., Pawlosky, R.J., Pusch, D.J.: Appl. Environ. Microbiol., **50**, 482-486 (1985)
3) Sugiura, Y., Watanabe, Y., Tanaka, T., Yamamoto, S., Ueno, Y.: Appl. Environ. Microbiol., **56**, 3047-3051 (1990)
4) Takahashi, M., Shibutani, M., Sugita-Konishi, Y., Aihara, M., Inoue, K., Woo, G.H., Fujimoto, H., Hirose, M.: Food Chem. Toxicol., **46**, 125-135 (2008)
5) Sugita-Konishi, Y., Park, B.J., Kobayashi-Hattori, K., Tanaka, T., Chonan, T., Yoshizawa, K., Kumagai, S.: Biosci. Biotechnol. Biochem., **70**, 1764-1768 (2006)
6) Kushiro, M.: Int. J. Mol. Sci., **9**, 2127-2145 (2008)
7) Young, J.C., Fulcher, R.G., Hayhoe, J.H., Scott, P.M., Dexter, J.E.: J. Agric. Food Chem., **32**, 659-664 (1984)
8) Samar, M.M., Neira, M.S., Resnik, S.L., Pacin, A.: Food Addit. Contam., **18**, 1004-1010 (2001)

国産小麦粉を含む原料を用いた食パンの製造過程におけるデオキシニバレノールとニバレノールの減衰率について

杉山圭一，鎌田洋一，小西良子：国立医薬品食品衛生研究所　衛生微生物部（158-8501　東京都世田谷区上用賀 1-18-1）
田中宏輝：サントリー株式会社　安全性科学センター（618-8503　大阪府三島郡島本町若山台 1-1-1）
田中敏嗣：神戸市環境保健研究所（650-0046　神戸市中央区港島中町 4-6）

ベーカリーにおいて国産小麦を含む原料で製造された食パン（35 検体）および同原料の小麦粉（12 検体）を入手し，各々の試料に含まれるデオキシニバレノール（DON）とニバレノール（NIV）の汚染量を LC-MS により分析した．その結果，小麦粉中からは DON および NIV は各々 31.3 ± 28.9，8.5 ± 3.7 μg/kg，食パン中からは各々 8.6 ± 5.1 μg/kg，3.4 ± 2.0 μg/kg が検出された．これより推測される食パン製造後の DON の残存率は約 74.4 %，NIV は 65.8 %であった．本結果は，食パンからのカビ毒摂取の実態に即したリスクアナリシスを実施するうえで貴重な情報となろう．

キーワード：デオキシニバレノール，ニバレノール，減衰，国産小麦粉，食パン

Contents lists available at ScienceDirect

Experimental and Toxicologic Pathology

journal homepage: www.elsevier.de/etp

Rapid deposition of glomerular IgA in BALB/c mice by nivalenol and its modifying effect on high IgA strain (HIGA) mice

Yasuaki Dewa [a,b], Sayaka Kemmochi [a,b], Masaomi Kawai [a,b], Yukie Saegusa [a,b], Tomoaki Harada [a], Keisuke Shimamoto [a,b], Kunitoshi Mitsumori [a], Susumu Kumagai [c], Yoshiko Sugita-Konishi [d], Makoto Shibutani [a,*]

[a] Laboratory of Veterinary Pathology, Tokyo University of Agriculture and Technology, 3-5-8 Saiwai-cho, Fuchu-shi, Tokyo 183-8509, Japan
[b] Pathogenetic Veterinary Science, United Graduate School of Veterinary Sciences, Gifu University, 1-1 Yanagido, Gifu 501-1193, Japan
[c] Department of Veterinary Medical Sciences, Graduate School of Agricultural and Life Sciences, The University of Tokyo, 1-1-1 Yayoi, Bunkyo-ku, Tokyo 113-8657, Japan
[d] Division of Microbiology, National Institute of Health Sciences, 1-18-1 Kamiyoga, Setagaya-ku, Tokyo 158-8501, Japan

ARTICLE INFO

Article history:
Received 7 June 2009
Accepted 1 September 2009

Keywords:
Nivalenol
IgA nephropathy
Glomerular mesangium
BALB/c mice
HIGA mice

ABSTRACT

To clarify the underlying mechanisms of IgA nephropathy (IgAN) induced by nivalenol (NIV), a trichothecene mycotoxin, we examined the time and dose relationships of glomerular deposition of IgA by NIV in BALB/c mice (Experiment 1), and also evaluated the modification of NIV on spontaneous IgAN in an inbred murine model, a high IgA strain (HIGA), during its early stage of pathogenesis (Experiment 2). In Experiment 1, female BALB/c mice were given a diet containing 0, 12, or 24 ppm concentration of NIV for 4 or 8 weeks. An increase in serum IgA levels was found at 24 ppm from 4 weeks. At week 8 of treatment, dose-dependent increases in serum IgA levels and glomerular deposition of IgA and IgG were observed without accompanying histopathological glomerular changes. On the other hand, in Experiment 2, control HIGA mice exhibited rather high levels of serum IgA as compared with BALB/c mice from 4 weeks of experiment as well as glomerular deposition of IgA and IgG and mesangial proliferation as revealed at week 8. NIV at 24 ppm further increased serum IgA in this strain; however, it did not enhance glomerular immunoglobulin deposition or histopathological lesion. These results suggest that NIV-induced increase of serum IgA levels may be primarily responsible for glomerular immunoglobulin deposition; however, NIV does not enhance glomerular IgA deposition that may lead to exacerbation of predisposed IgAN in the short term, irrespective of the further elevation of serum IgA from the high basal levels.

Introduction

Nivalenol (NIV) is a trichothecene mycotoxin produced by Fusarium fungi which, along with deoxynivalenol (DON), are frequently detected in agricultural commodities such as wheat, rye, barley, oats, and other cereals. Thus, contamination by these mycotoxins is a serious concern for human and animal health (Ali et al., 1998; Sudakin, 2003), and health risks associated with exposure to Fusarium mycotoxins need to be assessed. It is well-known that trichothecene mycotoxins induce various toxic effects in animals such as suppression of body growth and immune function, diarrhea, and general loss of condition. The more potent trichothecene mycotoxins, T-2 toxin and diacetoxyscirpenol, can induce severe toxicosis, including hemorrhage and necrosis in the gastrointestinal tract, with destruction of hematopoietic and lymphoid tissues and irritation of the skin and oral cavity (Ryu et al., 1988; Hascheck et al., 2002; SCF, 2002; Rocha et al., 2005). Moreover, trichothecenes affect immunological functions by deregulating production of cytokines and immunoglobulins and by inducing apoptosis (Thuvander et al., 1999; Bondy and Pestka, 2000; Pestka et al., 2004).

With regard to renal toxicity, dietary administration of NIV or DON to mice results in an elevation of serum IgA levels and its deposition in the glomerular mesangium (Hinoshita et al., 1997; Pestka et al., 1989), resembling IgA nephropathy (IgAN) in humans. Human IgAN is the most common primary chronic glomerulonephritis throughout the world (Berger and Hinglais, 1968; Tomino, 1999). Although IgAN is prevalent in all ethnic groups, Japan and Korea have some of the highest recorded incidences of this disorder. For example, approximately 50% of new cases of glomerulonephritis and 40% of all end-stage renal disease in Japan are estimated to be due to IgAN (Galla, 1995;

Abbreviations: DON, deoxynivalenol; HE, hematoxylin and eosin; HIGA mice, high IgA strain mice; IgAN, IgA nephropathy; NIV, nivalenol; PAS, periodic acid-Schiff; SLE, systemic lupus erythematosus; Th cell, T-helper cell

* Corresponding author. Tel.: +81 42 367 5874; fax: +81 42 367 5771.
E-mail address: mshibuta@cc.tuat.ac.jp (M. Shibutani).

0940-2993/$ - see front matter © 2009 Elsevier GmbH. All rights reserved.
doi:10.1016/j.etp.2009.09.002

Please cite this article as: Dewa Y, et al. Rapid deposition of glomerular IgA in BALB/c mice by nivalenol and its modifying effect on high IgA strain (HIGA) mice. Exp Toxicol Pathol (2009), doi:10.1016/j.etp.2009.09.002

D'Amico et al., 2001; Tumlin et al., 2007). Although the factors involved in the pathogenetic mechanisms of IgAN include environmental agents, genetic backgrounds, abnormality of the IgA1 molecule, and various inflammation mediators (Wada, et al., 2003), the precise mechanisms are still unclear.

Serum levels of IgA and IgA containing immune complexes have not fulfilled the expectations of providing useful tools for diagnosis and prognosis of IgAN in humans (Amore et al., 2006). In the present study, we wished to clarify the underlying mechanisms of NIV-induced IgAN with regard to the effect of increased serum IgA levels on the initiation or progression of IgAN. For this purpose, time and dose relationships of NIV treatment for the induction of glomerular IgA deposition were first examined using BALB/c mice (Experiment 1). The impact of NIV on the progression of IgAN was then analyzed in an inbred murine model of spontaneous IgAN using a high IgA strain (HIGA) mice (Muso et al., 1996) during its early stage of pathogenesis (Experiment 2).

Materials and methods

Chemicals

Nivalenol (NIV) used in this study was purified in the Division of Microbiology, National Institute of Health Sciences, Japan. For purification of NIV, Fusarenon X was extracted and purified from culture media of Fusarium kyushuense (Fn-2B). The identity and purity of NIV was determined by liquid chromatography/mass spectrometry (LC/MS; LCMS-2010A; Shimadzu Corp., Kyoto Japan), with an Atmospheric Pressure Chemical Ionization Interface and the LC system (LC-2010CHT; Shimadzu Corp.), and the purity was estimated to be $>98\%$ from the area percentage of the chromatogram (Kubosaki et al., 2008; Takahashi et al., 2008). For administration to mice, NIV was first dissolved in a small quantity of ethanol and then well mixed into powdered MF basal diet (Oriental Yeast Co., Tokyo, Japan). Stability of the test compound in the diet was confirmed for up to 2 weeks at room temperature ($>92\%$). Therefore, test diets were prepared every 2 weeks, and stored at 4 °C before use (Kubosaki et al., 2008; Takahashi et al., 2008).

Animals

In this study, female BALB/c Cr Slc mice and HIGA/Nsc Slc mice aged 5 weeks were purchased from Japan SLC Inc. (Shizuoka, Japan) and used as experimental animals in the NIV-induced and spontaneous IgAN models, respectively. They received a powdered MF diet and tap water *ad libitum*. Four animals were housed per polycarbonate cage with sterilized softwood chips as bedding in a barrier-maintained animal room conditioned at 22–26 °C and 52–61% humidity, on a 12-h light/dark cycle. After the 1 week acclimatization period, animals, weighing 17.53 ± 1.23 g (BALB/c mice; mean $\pm$ SD) and 25.52 ± 1.58 g (HIGA mice), were randomly divided into 3 groups (Experiments 1) and 2 groups (Experiment 2), respectively. Each group consists of 16 animals.

Experimental design

Experiment 1 was performed to examine the dose and time relationships for the induction of glomerular IgA deposition by NIV in the short term using BALB/c mice. BALB/c mice were given 0 (control), 12 or 24 ppm NIV in their powdered diet for a treatment period of 4 or 8 weeks. NIV at 12 ppm has been shown to elevate serum IgA levels and induce IgA deposits in the glomerular mesangium in C3H mice strain within 8 weeks (Hinoshita et al., 1997). Therefore, we chose the dose of 12 ppm as the first dose in this study, and the upper dose of 24 ppm was also selected to confirm the dose-dependency of NIV-induced glomerular IgA deposition. In Experiment 2, HIGA mice were given 0 (control) or 24 ppm NIV in their powdered diet for a treatment period of 4 or 8 weeks to evaluate the effect of NIV on the progression of spontaneous IgAN. The animals were observed daily for clinical signs and mortality, and body weights were measured every week during the study period. The amount of supplied and residual diet was weighed weekly to calculate the average daily consumption within each week, and then the overall mean throughout the treatment period was calculated from the determined weekly food consumption. At the end of the experiment, all animals were anesthetized with ether, weighed, and blood samples were collected from the abdominal vena cava for serum IgA and IgG determination. Animal care and experiments were carried out in accordance with the Guide for Animal Experimentation of Tokyo University of Agriculture and Technology.

Determination of immunoglobulin levels in serum

The blood samples collected at necropsy were centrifuged (1000g, 15 min) and sera obtained were stored at −80 °C. The levels of serum IgG and IgA antibodies were determined in 5–6 animals (4-week treatment) or 6–8 animals (8-week treatment) of

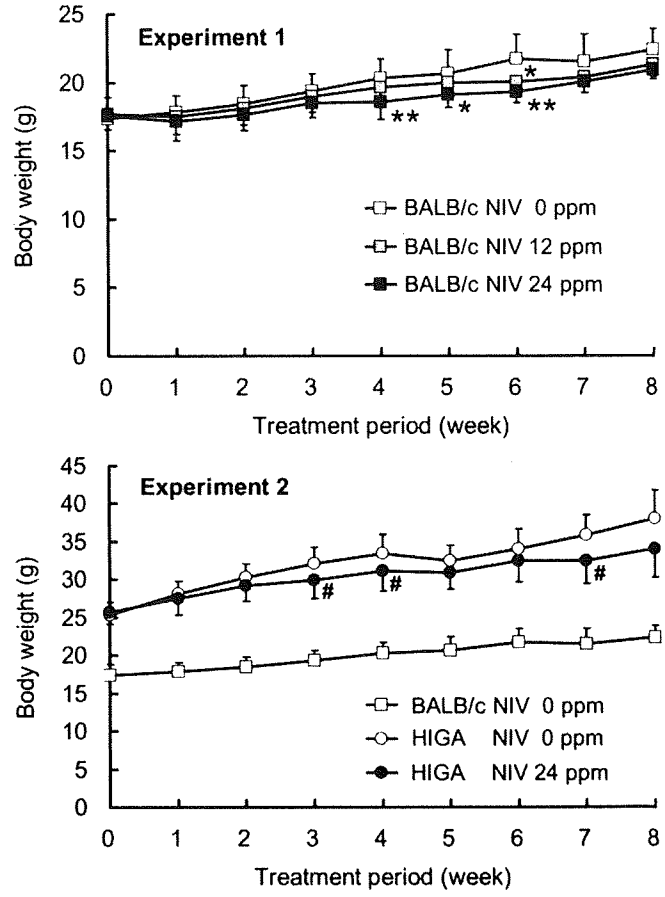

Fig. 1. Body weight curves for female mice of BALB/c and a high IgA strain (HIGA) given nivalenol (NIV) for 4 or 8 weeks. Data represent mean $\pm$ SD. $^{*}P < 0.05$ and $^{**}P < 0.01$, as compared with the untreated controls (Dunnett's test). $^{\#}P < 0.05$, as compared with the untreated HIGA mice (Tukey's multiple test). In Experiment 2, body weights of HIGA mice in each week were significantly higher than those of the age-matched control BALB/c mice ($^{\#}P < 0.01$; Tukey's multiple test).

Please cite this article as: Dewa Y, et al. Rapid deposition of glomerular IgA in BALB/c mice by nivalenol and its modifying effect on high IgA strain (HIGA) mice. Exp Toxicol Pathol (2009), doi:10.1016/j.etp.2009.09.002

each group by using a turbidimetric immunoassay at SRL, Inc. (Tokyo, Japan).

Histopathology and immunofluorescence

At necropsy, kidneys were removed and weighed and fixed in 10% buffered formalin or frozen in liquid nitrogen immediately after embedding in Tissue-Tek 4583 OCT compound (Sakura Finetek Japan, Tokyo, Japan). The formalin-fixed kidneys were routinely processed for paraffin embedding, sectioned, and subjected to hematoxylin and eosin (HE) or periodic acid-Schiff (PAS) staining. For immunofluorescence, frozen tissues from 8-week treatment of NIV were sectioned at 8 μm and fixed with ice-cold acetone at −20 °C for 5 min. Using an indirect immunofluorescence method for the detection of IgA and IgG, goat anti-mouse IgA or IgG (Kirkegaard and Perry Laboratories, Gaithersburg, MD, USA) antibodies were employed using a dilution of 1:1000 or 1:500 followed by incubation with fluorescein isothiocyanate conjugated anti-goat immunoglobulins (Dako, Glostrup, Denmark) with a dilution of 1:100. The fluorescence was detected with a confocal laser scanning microscope (Leica TCS NT, Leica Microsystems, Heidelberg, Germany). FITC was excited at 488 nm using an argon/krypton laser and the fluorescence was selected by a 530 nm band-pass filter. The emitted fluorescence signals were visualized by calculation of the average pixel value of 4 frame scans. For evaluation of the immunoreactivity of IgA and IgG in glomeruli, the intensity of fluorescence staining was visually scored as 0 (none), 1 (slight), 2 (moderate), or 3 (strong) by observation of 5 randomly selected areas including approximately 15 glomeruli/mice at a 200-fold magnification.

Statistics

Variance in data for body weights, serum IgA and IgG levels, and kidney weights (both absolute and relative weights) was checked for homogeneity by Bartlett's procedure. If the variance was homogeneous, the data were assessed by one-way analysis of variance. If not, the Kruskal–Wallis test was applied. When statistically significant differences were indicated, Dunnett's multiple test was employed for comparisons between the control and treatment groups (Experiment 1). In Experiment 2, when statistically significant differences were indicated by Bartlett's procedure, Tukey's multiple test (homogeneity) or the Steel–Dwass multiple test (non-homogeneity) was used for comparisons between the control BALB/c or HIGA mice and NIV-treated HIGA mice. The severity of immunoglobulin deposition in the glomerular tufts was compared using Mann–Whitney's *U*-test. Numerical data are presented as mean ± SD. A P value of less than 0.05 was considered statistically significant.

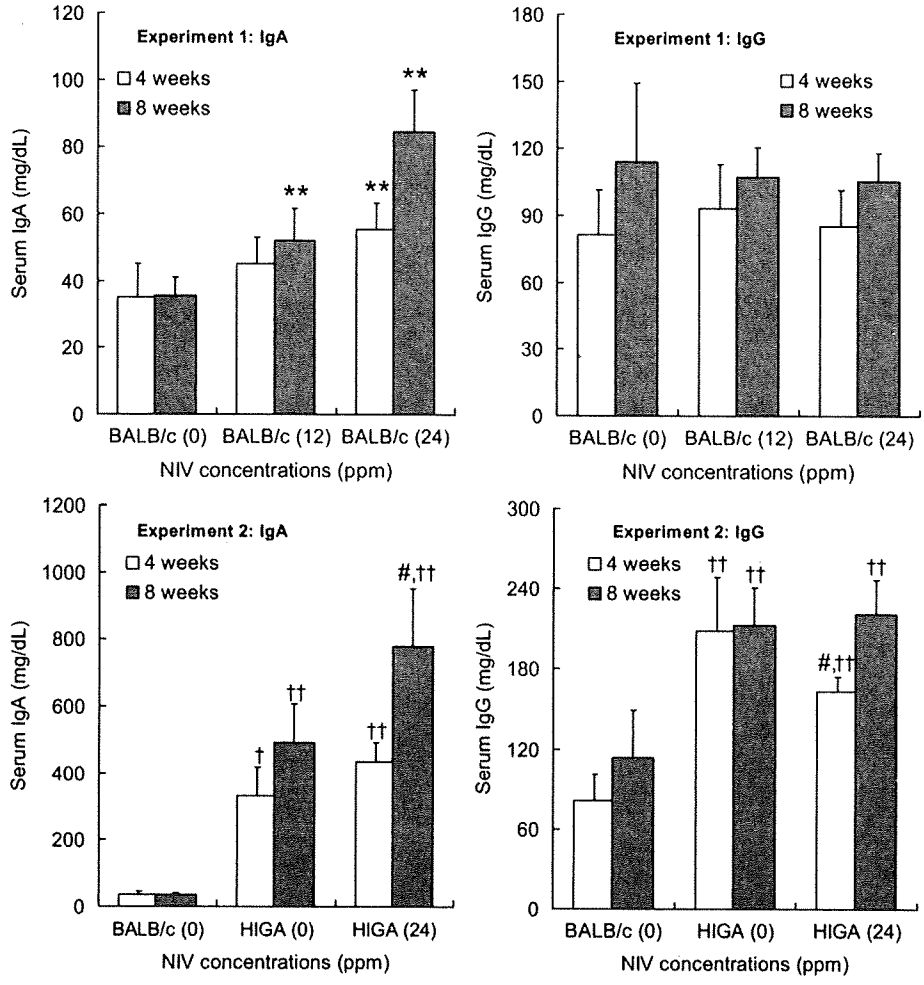

Fig. 2. Serum IgA and IgG levels in female mice of BALB/c and a high IgA strain (HIGA) given nivalenol (NIV) for 4 or 8 weeks. Data represent mean ± SD. $^{**}P < 0.01$, as compared with the untreated controls (Dunnett's test). $^{\#}P < 0.05$, as compared with the untreated HIGA mice (Tukey's multiple test). $^{\dagger}P < 0.05$ and $^{\dagger\dagger}P < 0.01$, as compared with the age-matched BALB/c mice (Tukey's or Steel–Dwass multiple test).

Please cite this article as: Dewa Y, et al. Rapid deposition of glomerular IgA in BALB/c mice by nivalenol and its modifying effect on high IgA strain (HIGA) mice. Exp Toxicol Pathol (2009), doi:10.1016/j.etp.2009.09.002

Results

In-life parameters

No deaths or clinical signs occurred during the experiments.

In Experiment 1, mean body weights of BALB/c mice were significantly decreased at 24 ppm NIV from weeks 4 to 6 and at 12 ppm NIV at week 6 of the feeding experiment (Fig. 1). With regard to food consumption, although values were approximate due to a small number of samples in each group

Table 1
Final body and kidney weights of BALB/c and a high IgA strain (HIGA) mice given a diet containing nivalenol (NIV) for 4 or 8 weeks.

Strain	Nivalenol (ppm)	Duration (weeks)	No. of animals	Final body weight (g)	Kidney weights	
					Absolute (g)	Relative (%)
BALB/c	0	4	8	20.21 ± 0.96	0.276 ± 0.022	1.36 ± 0.07
	12	4	8	19.88 ± 1.83	0.266 ± 0.020	1.34 ± 0.08
	24	4	8	18.79 ± 1.31	0.251 ± 0.019	1.33 ± 0.03
	0	8	8	22.36 ± 1.54	0.295 ± 0.027	1.32 ± 0.08
	12	8	8	21.32 ± 0.87	0.284 ± 0.010	1.33 ± 0.05
	24	8	8	20.94 ± 0.70*	0.272 ± 0.015	1.30 ± 0.05
HIGA	0	4	8	34.46 ± 2.71††	0.370 ± 0.031††	1.07 ± 0.07††
	24	4	8	31.51 ± 3.10††	0.373 ± 0.017††	1.19 ± 0.14†,#
	0	8	8	37.95 ± 3.73††	0.434 ± 0.042††	1.14 ± 0.04††
	24	8	8	34.07 ± 3.83††	0.429 ± 0.034††	1.27 ± 0.10#

*$P < 0.05$: Significantly different from control BALB/c mice (Dunnett's multiple test).
†$P < 0.05$, ††$P < 0.01$: Significantly different from control BALB/c mice (Tukey's multiple test).
#$P < 0.05$: Significantly different from control HIGA mice (Tukey's multiple test).

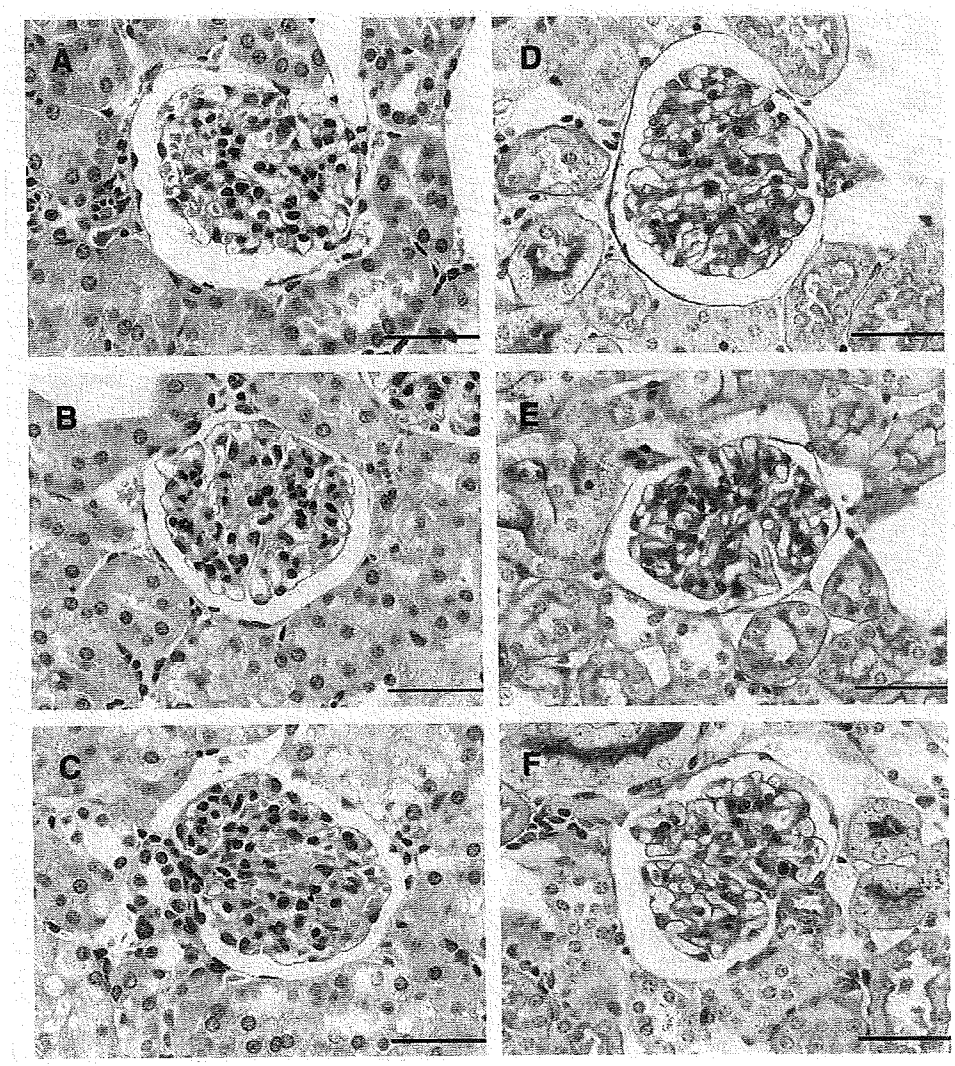

Fig. 3. Histopathology of the kidneys with hematoxylin and eosin (HE; A–C) and periodic acid-Schiff (PAS; D–F) stains in BALB/c mice given nivalenol (NIV) for 8 weeks in Experiment 1. Control BALB/c mice (A, D); BALB/c mice given 12 ppm (B, E) or 24 ppm (C, F) NIV. Original magnification: 400 ×. Bar=50 μm.

Please cite this article as: Dewa Y, et al. Rapid deposition of glomerular IgA in BALB/c mice by nivalenol and its modifying effect on high IgA strain (HIGA) mice. Exp Toxicol Pathol (2009), doi:10.1016/j.etp.2009.09.002

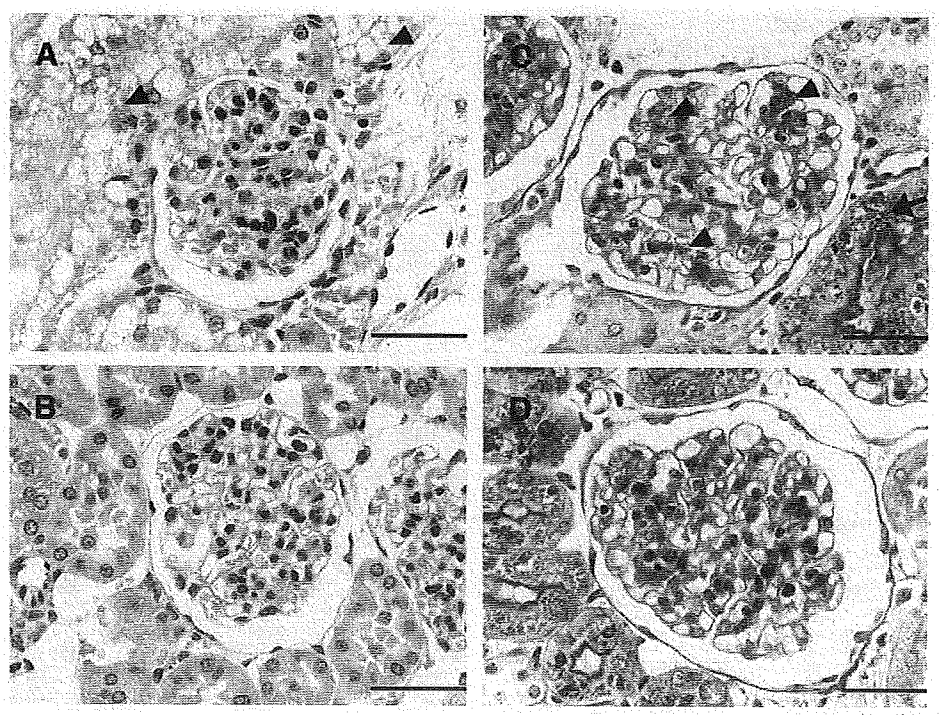

Fig. 4. Histopathology of the kidneys with hematoxylin and eosin (HE; A, B) and periodic acid-Schiff (PAS; C, D) stains in HIGA mice given NIV for 8 weeks in Experiment 2. Control HIGA mice (A, C); HIGA mice given 24 ppm NIV (B, D). In both control and NIV-treated mice, a slight increase in mesangial proliferation (arrowheads in panel C) and vacuolar degeneration of renal tubules (arrowheads in panel A) as well as an increase in PAS-positive granular deposits in the tubular cytoplasm (arrow in panel C) are observed. Original magnification: 400 ×. Bar=50 μm.

(n=2 or 4 cages/group; data not statistically analyzed), there were no obvious changes (data not shown). In Experiment 2, mean body weight in HIGA mice treated with 24 ppm NIV was decreased throughout the feeding period and was statistically significant at weeks 3, 4, and 7 of the experiment (Fig. 1). No obvious changes were observed in the food consumption.

Serum immunoglobulin levels

Serum IgA and IgG levels are shown in Fig. 2. In Experiment 1, serum IgA levels were significantly increased after a 4-week treatment of 24 ppm NIV, and there was a significant dose-dependent increase by 8 weeks of treatment (52.2 ± 9.5 mg/dL at 12 ppm and 84.6 ± 12.5 mg/dL at 24 ppm) compared with the controls (35.7 ± 5.4 mg/dL); however, serum IgG levels were not affected by NIV treatment. In Experiment 2, both serum IgA and IgG levels in HIGA mice were significantly higher than those in the age-matched control BALB/c mice, irrespective of NIV treatment. Fold increases of HIGA mice relative to BALB/c mice were 9.5 or 13.8 in IgA, and 2.6 or 1.9 in IgG at 9 or 13 weeks of age, respectively. NIV treatment enhanced serum IgA levels by 8 weeks (492.6 ± 115.3 vs. 780.3 ± 171.2 mg/dL, $P < 0.05$). On the other hand, serum IgG levels were decreased by 4 weeks of NIV treatment.

Body and organ weights

Data for the final body and organ weights are shown in Table 1.

In Experiment 1, body weight was significantly decreased at 8 weeks of 24 ppm NIV treatment. No significant changes were observed in kidney weight, irrespective of the dose and duration of NIV treatment. In Experiment 2, mean body weight in HIGA mice was significantly higher than that in the age-matched control BALB/c mice. The effect of NIV treatment on final body weight in HIGA mice was less apparent, showing a tendency to decrease at weeks 4 and 8 of NIV treatment; however, the relative weight of the kidney was significantly increased by 24 ppm NIV at 4 and 8 weeks of treatment (Table 1).

Histopathology and immunofluorescent analysis

Histopathological views of the kidney using HE and PAS stains are shown in Figs. 3 and 4. Representative views of glomerular depositions of IgA and IgG, and their quantitative data are shown in Figs. 5 and 6, respectively.

In Experiment 1, there were no apparent histopathological changes in the kidneys of BALB/c mice at both 12 and 24 ppm NIV at 4 or 8 weeks of treatment (Fig. 3). However, immunofluorescence analysis showed that the degree of glomerular deposition of IgA and IgG in NIV-treated animals was significantly increased compared with the controls (from grade 0 to grade 1 or 2; Figs. 5 and 6). Moreover, this deposition was also increased with an increase in dose of NIV (from grade 2 to grade 3 or 4).

In Experiment 2, a slight increase in mesangial proliferation and vacuolar degeneration of renal tubules as well as an increase in PAS-positive granular deposits in the tubular cytoplasm were observed in the kidneys of HIGA mice compared with age-matched control BALB/c mice (Figs. 3 and 4). The grade of IgA as well as IgG depositions was significantly increased compared with control BALB/c mice (from grade 0 to grade 2 or 3; $P < 0.01$), and these depositions were observed diffusely in the mesangial area (Figs. 5 and 6). However, the effect of NIV treatment on these depositions was not apparent with the dose and treatment period employed.

Discussion

Our results showed that 24 ppm NIV increased serum IgA levels from week 4, and caused dose-related increases of serum

Please cite this article as: Dewa Y, et al. Rapid deposition of glomerular IgA in BALB/c mice by nivalenol and its modifying effect on high IgA strain (HIGA) mice. Exp Toxicol Pathol (2009), doi:10.1016/j.etp.2009.09.002

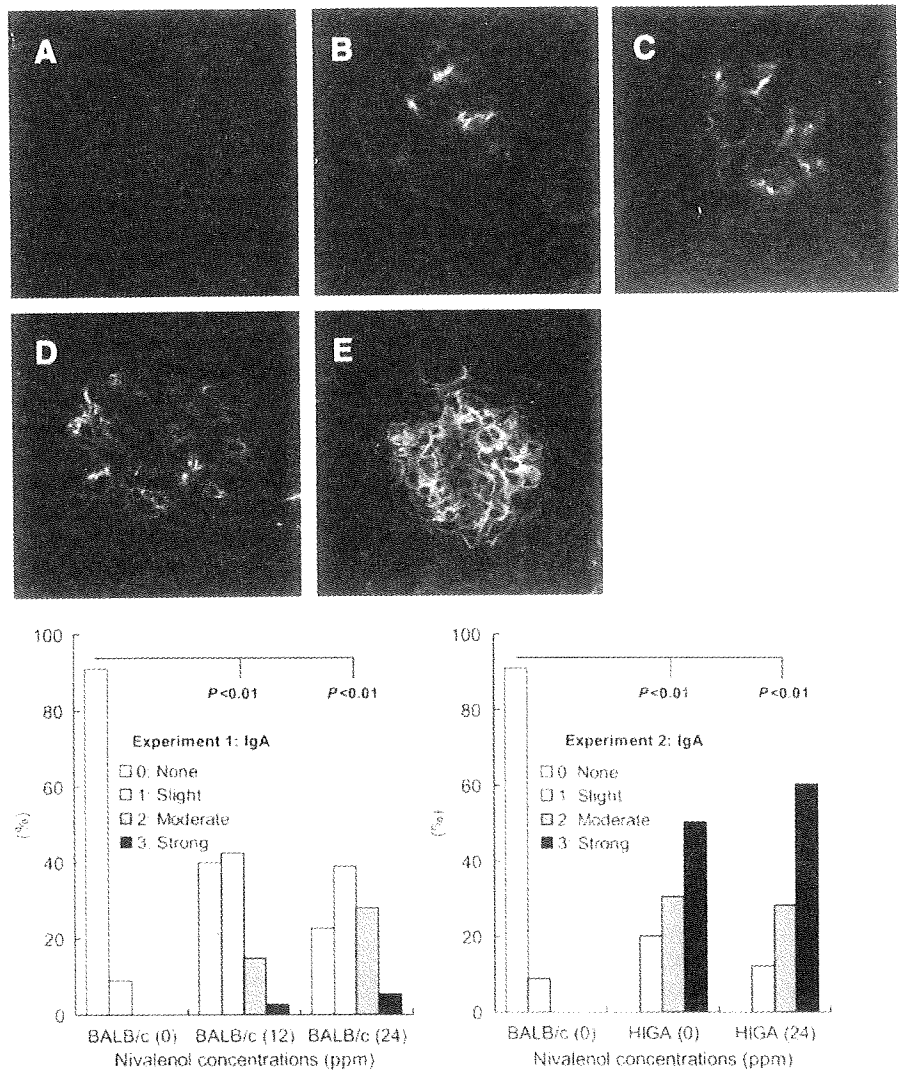

Fig. 5. Glomerular IgA deposition in the kidneys of BALB/c and a high IgA strain (HIGA) mice given nivalenol (NIV) for 8 weeks. Control BALB/c mice (A); BALB/c mice given 12 ppm (B) or 24 ppm (C) of NIV; control HIGA mice (D); HIGA mice given 24 ppm of NIV (E). The intensity of fluorescence for IgA in each group was scored as 0 (none), 1 (slight), 2 (moderate), or 3 (strong). NIV treatment significantly increased the severity of IgA deposition in the glomerular tufts with increasing doses in BALB/c mice. Glomerular IgA deposition in HIGA mice was also higher than that of the age-matched control BALB/c mice ($P < 0.01$; Mann–Whitney's U-test).

IgA levels and glomerular deposition of IgA and IgG by week 8, which is consistent with a previous report by Hinoshita et al. (1997) using C3H mice strains. On the other hand, serum IgG levels were unchanged in the BALB/c strain in the present study, which is in contrast to an increase in the C3H strain in the previous study. With regard to the deposition of IgA in glomerular mesangium, virus-induced experimental IgAN models have shown that BALB/c mice are genetically prone to shift T-helper (Th) 2 immune responses and that this T cell cytokine polarity is a determinant of reduction in terminal galactosylation and sialylation of IgA (Chintalacharuvu et al., 2001, 2008), which is recognized as an important pathogenic factor in glomerular IgA deposition (Allen et al., 1995; Hiki et al., 1996). However, the treatment dose and duration of NIV used in the present study did not show any histopathological renal changes. In humans, IgAN is the most common primary chronic nephropathy, and histopathological changes characterized by expansion of glomerular mesangial matrix and mesangial proliferation develop after the long period of disease process (Tomino, 2008). Even with HIGA strain mice, onset of glomerular injury differs between mice with an early onset group requiring at least 20 weeks (Tomino, 2008). Therefore, immunoglobulin deposition without accompanying histological alterations observed here might reflect an early stage of IgAN. Collectively, BALB/c mice are also a sensitive strain for induction of NIV-induced glomerular deposition of IgA. This strain of mice (females) is also known to be sensitive to dietary DON to induce IgAN accompanied with increased serum IgA concentration (Greene et al., 1994).

Although the etiology of IgAN in humans remains unclear, several factors have been suggested to provoke the exacerbation of IgAN. These factors include infectious agents such as Sendai virus (Jessen et al., 1987) and Coxsackie B4 virus (Kawasaki et al., 2006) or food antigens/contaminants such as ovalbumin (Coppo, 1988) and vomitoxin DON (Yan et al., 1998). Up to 60% of patients with IgAN were reported to develop episodes of hematuria and variable proteinuria in close temporal association with acute upper respiratory or gastrointestinal syndromes, suggestive of an affect by exogenous agents (Chintalacharuvu et al., 2001; D'Amico et al., 2001). Therefore, besides a role for causative factors (Hinoshita et al., 1997), dietary contaminated NIV could exacerbate IgAN in humans. An HIGA strain of mice was established as an inbred murine model of IgAN, and these mice

Please cite this article as: Dewa Y, et al. Rapid deposition of glomerular IgA in BALB/c mice by nivalenol and its modifying effect on high IgA strain (HIGA) mice. Exp Toxicol Pathol (2009), doi:10.1016/j.etp.2009.09.002

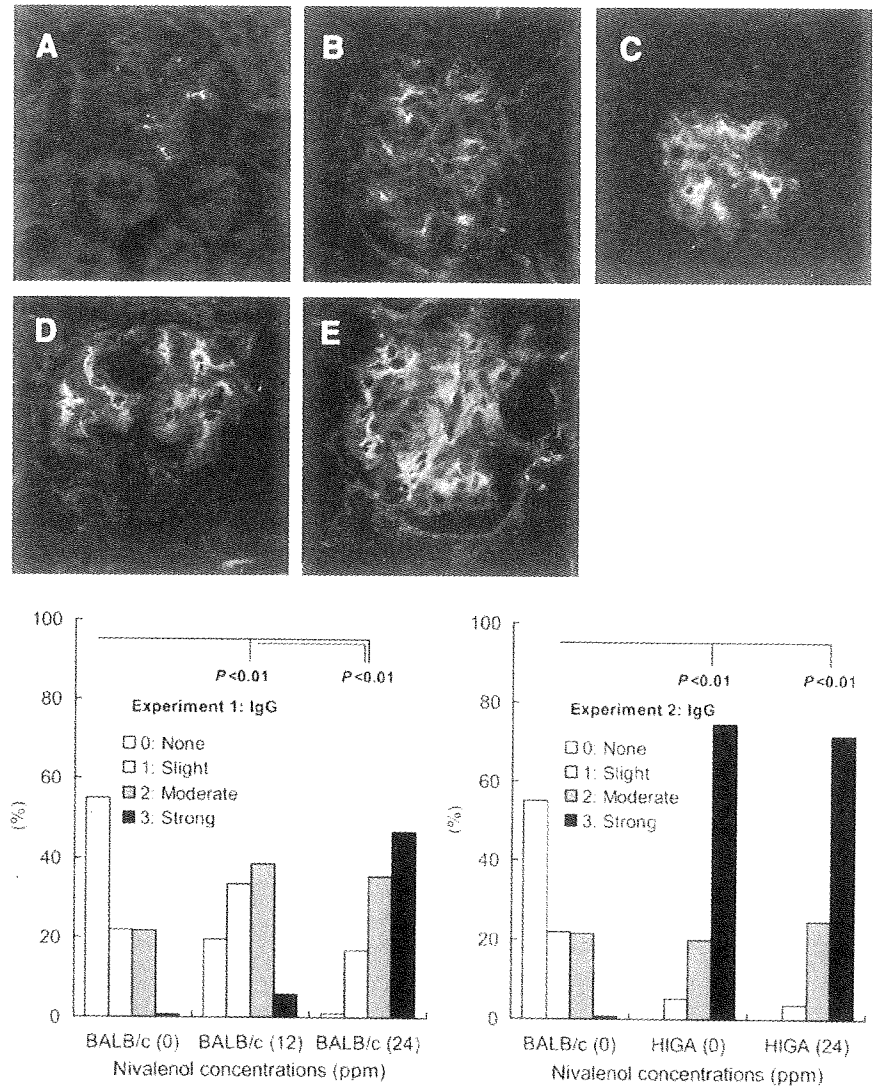

Fig. 6. Glomerular IgG deposition in the kidneys of BALB/c and a high IgA strain (HIGA) mice given nivalenol (NIV) for 8 weeks. Control BALB/c mice (A); BALB/c mice given 12 ppm (B) or 24 ppm (C) of NIV; control HIGA mice (D); HIGA mice given 24 ppm of NIV (E). The intensity of fluorescence for IgG in each group was scored as 0 (none), 1 (slight), 2 (moderate), or 3 (strong). NIV treatment significantly increased the severity of IgG deposition in the glomerular tufts with increasing doses in BALB/c mice. Glomerular IgG deposition in HIGA mice was also higher than that of the age-matched control BALB/c mice ($P < 0.01$; Mann–Whitney's U-test).

exhibited constantly high serum levels of IgA from 10 to 60 weeks of age with polymeric IgA-dominant mesangial deposition and enhanced extracellular matrix accumulation (Muso et al., 1996; Miyawaki et al., 1997). Therefore, in the present study, HIGA mice were used to evaluate the possibility that NIV accelerates the progression of spontaneous IgAN. Our results confirmed that serum IgA levels were significantly increased with treatment of NIV compared with untreated HIGA mice. However, the enhancing effect of NIV on IgAN was not pathologically evident with 24 ppm NIV treatment for 8 weeks. These results may suggest that NIV treatment does not exacerbate the deposition, irrespective of increased serum IgA levels.

Interestingly, DON treatment of 3 strains of mice predisposed to systemic lupus erythematosus (SLE) did not increase serum immunoglobulins, but, among them, only one strain of mice (BXSB mice) showed increased mesangial deposition of IgA, IgG, and complement C_3 (Banotai et al., 1999). Authors suggested that subtle effects on IgA production occur at the lymphocyte level, but that this was not sufficient to alter systemic levels, reflecting a lower sensitivity of these SLE mice to the effects of DON. They also suggested that strain difference in the glomerular deposition may be due to the difference in the type of IgA secreted, i.e., monomeric vs. polymeric, for the capacity to mediate immune complex formation. Further studies should therefore examine effects of NIV on the size of secreted IgA in HIGA mice in the present study.

It is generally accepted that the production of IgA is dependent on its release from activated Th2 cells of cytokines such as interleukin (IL)-4, IL6, and IL10 (Xu-Amano et al., 1993; Harriman et al., 1988; Okahashi et al., 1996). NIV has been shown to stimulate Th2 cells to produce cytokines that may eventually lead to IgA hyperproduction (Pestka and Bondy, 1989). Nogaki et al. (2000) suggested a pathogenic role of T cell function and a fluctuation of T cell subsets, especially Th1 and Th2 balance, and that this is crucial for the immunopathological phenotype of glomerular lesions in HIGA mice. Thus, Th1 is predominant at a younger age, but the Th2 population takes place in later age by an increase in transforming growth factor-β1 in helper T cells. The authors have speculated that the Th1 may be related to a progression of inflammatory renal lesions, while Th2 may contribute to increased IgA production, leading to glomerular IgA deposition and progressive glomerulosclerosis

Please cite this article as: Dewa Y, et al. Rapid deposition of glomerular IgA in BALB/c mice by nivalenol and its modifying effect on high IgA strain (HIGA) mice. Exp Toxicol Pathol (2009), doi:10.1016/j.etp.2009.09.002

(Nogaki et al., 2000). However, basal Th2 function may be high in HIGA mice, even at a younger age, because we found glomerular deposition of IgA as well as very high serum IgA levels compared with the age-matched BALB/c mice. Moreover, NIV treatment for 8 weeks efficiently increased IgA production in HIGA mice reflecting enhanced Th2 activity irrespective of a predominance of the Th1 population at a younger age. However, profound increase of serum IgA by NIV did not enhance subsequent glomerular deposition of IgA in the short term. Although the corresponding mechanism for the lack of enhancement of predisposed IgAN is not clear, the polarity shift between Th1 and Th2 immune responses affects the pattern of IgA glycosylation and exerts direct or indirect effects on functional glomerular responses to immune complex deposition (Chintalacharuvu et al., 2008).

In conclusion, dietary exposure of NIV in BALB/c mice increased serum IgA levels starting as early as 4 weeks of treatment and resulted in deposition of IgA and IgG at week 8 of treatment, indicating that the effect of NIV to increase serum IgA levels may be responsible for development of subsequent glomerular IgA deposition in the short term. In HIGA mice, NIV increased serum IgA levels, but it did not have any effect on glomerular deposition of IgA and IgG, suggesting that NIV does not enhance glomerular IgA deposition that may lead to exacerbation of predisposed IgAN in the short term, irrespective of increased serum IgA levels. Although further studies are needed with regard to the mechanisms of glomerular deposition of IgA, as well as determining the immunomodulatory profile of NIV in the onset of IgAN, our results provide useful information for establishing an evaluation platform for the prevention and treatment of IgAN.

Acknowledgments

This work was supported by Health and Labour Sciences Research Grants (Research on Food Safety) from the Ministry of Health, Labour and Welfare of Japan. All authors disclose that there are no conflicts of interest that could inappropriately influence the outcome of the present study.

References

Ali NS, Yamashita A, Yoshizawa T. Natural co-occurrence of aflatoxins and Fusarium mycotoxins (fumonisins, deoxynivalenol, nivalenol and zearalenone) in corn from Indonesia. Food Addit Contam 1998;15:377–84.

Allen AC, Harper SJ, Feehally J. Galactosylation of *N*- and *O*-linked carbohydrate moieties of IgA1 and IgG in IgA nephropathy. Clin Exp Immunol 1995;100:470–4.

Amore A, Monteiro R, Coppo R. Immunoglobulin A (IgA) and its cellular receptors: recent advances and new pathogenetical hypothesis (in Italian). G Ital Nefrol 2006;23:313–22.

Banotai C, Azcona-Olivera JI, Greene-McDowelle DM, Pestka JJ. Effects of vomitoxin ingestion on murine models for systemic lupus erythematosus. Food Chem Toxicol 1999;37:533–43.

Berger J, Hinglais N. Intercapillary deposits of IgA–IgG. J Urol Nephrol 1968;74: 694–5.

Bondy GS, Pestka JJ. Immunomodulation by fungal toxins. J Toxicol Environ Health B Crit Rev 2000;3:109–43.

Chintalacharuvu SR, Nagy NU, Sigmund N, Nedrud JG, Amm ME, Emancipator. T cell cytokines determine the severity of experimental IgA nephropathy by regulating IgA glycosylation. Clin Exp Immunol 2001;126:326–33.

Chintalacharuvu SR, Yamashita M, Bagheri N, Blanchard TG, Nedrud JG, Lamm ME, et al. T cell cytokine polarity as a determinant of immunoglobulin A (IgA) glycosylation and the severity of experimental IgA nephropathy. Clin Exp Immunol 2008;153:456–62.

Coppo R. The pathogenetic potential of environmental antigens in IgA nephropathy. Am J Kidney Dis 1988;12:420–4.

D'Amico G, Napodano P, Ferrario F, Rastaldi MP, Arrigo G. Idiopathic IgA nephropathy with segmental necrotizing lesions of the capillary wall. Kidney Int 2001;59:682–92.

Galla JH. IgA nephropathy. Kidney Int 1995;47:377–87.

Greene DM, Bondy GS, Azcona-Olivera JI, Pestka JJ. Role of gender and strain in vomitoxin-induced dysregulation of IgA production and IgA nephropathy in the mouse. J Toxicol Environ Health 1994;43:37–50.

Hascheck WM, Voss KA, Beasley VR. Selected mycotoxins affecting animals and human health. In: Hascheck W, Rousseaux C, Wallig M, editors. Handbook of toxicologic pathology, vol. 1. Academic Press; 2002. p. 645–700.

Harriman GR, Kunimoto DR, Elliott JF, Paetkau V, Strober W. The role of IL-5 in IgA B cell differentiation. J Immunol 1988;140:303–27.

Hiki Y, Iwase H, Kokubo T, Horii A, Tanaka A, Nishikido J, et al. Association of asialo-galactosyl beta 1-3*N*-acetylgalactosamine on the hinge with a conformational instability of Jacalin-reactive immunoglobulin A1 in immunoglobulin A nephropathy. J Am Soc Nephrol 1996;7:955–60.

Hinoshita F, Suzuki Y, Yokoyama K, Hara S, Yamada A, Ogura Y, et al. Experimental IgA nephrophathy induced by a low-dose environmental mycotoxin, nivarenol. Nephron 1997;75:469–78.

Jessen RH, Nedrud JG, Emancipator SN. A mouse model of IgA nephropathy induced by Sendai virus. Adv Exp Med Biol 1987;216B:1609–18.

Kawasaki Y, Mitsuki H, Isome M, Nozawa R, Suzuki H. Renal effects of Coxsackie B4 virus in hyper-IgA mice. J Am Soc Nephrol 2006;17:2760–9.

Kubosaki A, Aihara M, Park BJ, Sugiura Y, Shibutani M, Hirose M, et al. Immunotoxicity of nivalenol after subchronic dietary exposure to rats. Food Chem Toxicol 2008;46:253–8.

Miyawaki S, Muso E, Takeuchi E, Matsushima H, Shibata Y, Sasayama S, Yoshida H. Selective breeding for high serum IgA levels from noninbred ddY mice: isolation of a strain with an early onset of glomerular IgA deposition. Nephron 1997;76:201–7.

Muso E, Yoshida H, Takeuchi E, Yashiro M, Matsushima H, Oyama A, et al. Enhanced production of glomerular extracellular matrix in a new mouse strain of high serum IgA ddY mice. Kidney Int 1996;50:1946–57.

Nogaki F, Muso E, Kobayashi I, Kusano H, Shirakawa K, Kamata, et al. Interleukin 12 induces crescentic glomerular lesions in a high IgA strain of ddY mice, independently of changes in IgA deposition. Nephrol Dial Transplant 2000;15: 1146–54.

Okahashi N, Yamamoto M, Vancott JL, Chatfield SN, Roberts M, Bluethmann H, et al. Oral immunization of interleukin-4 (IL-4) knockout mice with a recombinant Salmonella strain or cholera toxin reveals that CD4 Th2 cells producing IL-6 and IL-10 are associated with mucosal immunoglobulin A responses. Infect Immun 1996;64:1516–25.

Pestka JJ, Bondy GS. Alteration of immune function following dietary mycotoxin exposure. Can J Physiol Pharmacol 1989;68:1009–16.

Pestka JJ, Moorman MA, Warner RL. Dysregulation of IgA production and IgA nephropathy induced by the trichothecene vomitoxin. Food Chem Toxicol 1989;27:361–8.

Pestka JJ, Zhou HR, Moon Y, Chung YJ. Cellular and molecular mechanisms for immune modulation by deoxynivalenol and other trichothecenes: unraveling a paradox. Toxicol Lett 2004;153:61–73.

Rocha O, Ansari K, Doohan FM. Effects of trichothecene mycotoxins on eukaryotic cells: a review. Food Addit Contam 2005;22:369–78.

Ryu JC, Ohtsubo K, Izumiyama N, Nakamura K, Tanaka T, Yamamura H, et al. The acute and chronic toxicities of nivalenol in mice. Fundam Appl Toxicol 1988;11:38–47.

SCF (Scientific Committee for Food). Opinion on Fusarium toxins. Part 6: Group evaluation of T-2 toxin, HT-2 toxin, nivalenol and deoxynivalenol. 2002; Available at: < http://ec.europa.eu/food/fs/sc/scf/out123_en.pdf#search =%22SCF%202002%20nivalenol%22 > .

Sudakin DL. Trichothecenes in the environment: relevance to human health. Toxicol Lett 2003;143:97–107.

Takahashi M, Shibutani M, Sugita-Konishi Y, Aihara M, Inoue K, Woo GH, et al. 90-day subchronic toxicity study of nivalenol, a trichothecene mycotoxin, in F344 rats. Food Chem Toxicol 2008;46:125–35.

Thuvander A, Wikman C, Gadhasson I. In vitro exposure of human lymphocytes to trichothecenes: individual variation in sensitivity and effects of combined exposure on lymphocyte function. Food Chem Toxicol 1999;37:639–48.

Tomino Y. IgA nephropathy. From molecules to men. Contrib Nephrol 1999;126: 1–15.

Tomino Y. IgA nephropathy: lessons from an animal model, the ddY mouse. J Nephrol 2008;21:463–7.

Tumlin JA, Madaio MP, Hennigar R. Idiopathic IgA nephropathy: pathogenesis, histopathology, and therapeutic options. Clin J Am Soc Nephrol 2007;2: 1054–61.

Wada J, Sugiyama H, Makino H. Pathogenesis of IgA nephropathy. Semin Nephrol 2003;23:556–63.

Xu-Amano J, Kiyono H, Jackson RJ, Staats HF, Fujihashi K, Burrows PD, et al. Helper T cell subsets for immunoglobulin A responses: oral immunization with tetanus toxoid and cholera toxin as adjuvant selectively induces Th2 cells in mucosa associated tissues. J Exp Med 1993;178:1309–20.

Yan D, Rumbeiha WK, Pestka JJ. Experimental murine IgA nephropathy following passive administration of vomitoxin-induced IgA monoclonal antibodies. Food Chem Toxicol 1998;36:1095–106.

Please cite this article as: Dewa Y, et al. Rapid deposition of glomerular IgA in BALB/c mice by nivalenol and its modifying effect on high IgA strain (HIGA) mice. Exp Toxicol Pathol (2009), doi:10.1016/j.etp.2009.09.002

RAPID COMMUNICATIONS IN MASS SPECTROMETRY
Rapid Commun. Mass Spectrom. 2009; **23**: 3119–3124
Published online in Wiley InterScience (www.interscience.wiley.com) DOI: 10.1002/rcm.4233

RCM

Determination of nivalenol and deoxynivalenol by liquid chromatography/atmospheric pressure photoionization mass spectrometry

Hiroki Tanaka[1]*†, Masahiko Takino[2], Yoshiko Sugita-Konishi[1], Toshitsugu Tanaka[3], Akira Toriba[4] and Kazuichi Hayakawa[4]

[1]National Institute of Health Sciences, 1-18-1 Kamiyoga, Setagaya-ku, Tokyo 158-8501, Japan
[2]Agilent Technologies Japan, Ltd., Hachioji Site 9-1, Takakura-cho, Hachioji-shi, Tokyo 192-8501, Japan
[3]Kobe Institute of Health, 4–6 Minatojima-Nakamachi, Chuo-ku, Kobe 650-0046, Japan
[4]Institute of Medical, Pharmaceutical and Health Sciences, Kanazawa University, Kakuma-machi, Kanazawa 920-1192, Japan

Received 7 June 2009; Revised 28 July 2009; Accepted 30 July 2009

Fusarium **species, a plant pathogenic fungus of wheat and other cereals, produces toxic metabolites such as nivalenol (NIV) and deoxynivalenol (DON). Control of contamination by these toxins is very difficult, and a continuous survey of the occurrence is necessary for these toxins. Thus, the accurate and convenient determination of the cereals contaminated with these toxins is important for the supply of safe foods. A selective analytical method based on high-performance liquid chromatography, combined with atmospheric pressure photoionization (APPI) mass spectrometry, has been developed for simultaneous determination of NIV and DON. The parameters investigated for the optimization of APPI were the ion source parameters fragmentor voltage, capillary voltage, and vaporizer temperature, and also mobile phase composition and flow rate. Furthermore, chemical noise and signal suppression of analyte signals due to sample matrix interference were investigated for APPI. The results indicated that APPI provides lower matrix effect and the correlation coefficient of NIV and DON in the range 0.2–100 ng · mL^{-1} was above 0.999. Recoveries of NIV and DON in wheat ranged from 86 to 107% and limits of detection of NIV and DON were 0.20 ng · g^{-1} and 0.39 ng · g^{-1}, respectively. In addition, the proposed method was applied for the analysis of naturally contaminated wheat samples. APPI was found to offer lower matrix effect and was a convenient technique for routine analysis of NIV and DON residues in wheat at trace levels. Copyright © 2009 John Wiley & Sons, Ltd.**

Trichothecene mycotoxins, such as nivalenol (NIV) and deoxinivalenol (DON), belong to the secondary metabolites produced by various filamentaneous fungi, such as *Fusarium*, *Myrothecium*, *Stachybotrys* and *Trichothecium*. Contamination of cereals with these toxins has caused several outbreaks of intoxications in human and animal populations. These contaminations were serious problems from the viewpoint of food safety, and there have been many reports of the natural occurrence of NIV and DON.[1–6] In particular, both NIV and DON have been detected in cereals and foodstuffs in Japan,[7,8] Korea,[8,9] Canada,[8] and so on. In contrast, these toxins possess a potent cytotoxicity to eukaryotic cells, and this biological activity is closely related to their lethal toxicity, dermal toxicity, cellular damage to actively dividing cells, impairment of immunoresponses, and inhibition of macromolecule syntheses.[10] Moreover. Takahashi *et al.*[11] have reported that NIV can modulate the immune system by subchronic dietary exposure, and that this modulation has a direct toxic effect on the lymphocytes. The Joint FAO/WHO Expert Committee on Food Additives (JECFA) established a level of 1 μg·kg^{-1} of body weight per day as the provisional maximum tolerable daily intake (PMTDI) for DON in 2001.[12] In line with this, the Ministry of Health, Labor and Welfare of Japan recommended a level of 1.1 mg·kg^{-1} of DON in wheat as the provisional standard for local governments in 2002. Equally, temporary TDI were proposed by the European Science Committee as 0.7 μg·kg^{-1} of body weight per day for NIV.[13] Thus, when the potential food safety problem and their various toxic effects are grasped, the accurate and convenient determination of the cereals contaminated with these toxins is important for the supply of safe foods. Therefore, to ensure food safety, a rapid and reliable method is needed for simultaneous identification and quantitation of NIV and DON in cereals.

Several analytical methods have been developed for the determination of NIV and DON in cereals. Gas chromatography and high-performance liquid chromatography (HPLC) are common techniques for the detection of these mycotoxins for both official and laboratory uses.[14–21] However, chemical

*Correspondence to: H. Tanaka, Research Center, Suntory Business Expert Ltd., 1-1-1 Wakayamadai, Shimamoto-cho, Mishima-gun, Osaka 618-8503, Japan.
E-mail: hiroki.t@poem.ocn.ne.jp
† Present address: Research Center, Suntory Business Expert Ltd., 1-1-1 Wakayamadai, Shimamoto-cho, Mishima-gun, Osaka 618-8503, Japan.

derivatization might introduce sample loss and interfering peaks, and also reduce the speed of the analytical procedure. Moreover, the use of HPLC with UV detection for the determination of NIV and DON has also some sensitivity limitations due to the lack of characteristic UV absorption of these molecules.

Recently, the liquid chromatography/mass spectrometry (LC/MS) technique has been introduced to determine some mycotoxins. This technique is very sensitive, selective and specific. Therefore, the high selectivity and the high sensitivity of MS detection methods combined with the resolving power of LC provide decisive advantages to perform qualitative as well as quantitative analysis of a wide range of molecules at trace levels. So far, several types of interface for LC/MS have been reported for the analysis of NIV or DON.[14–16,22–25] Especially, atmospheric pressure ionization (API) interfaces, represented by atmospheric pressure chemical ionization (APCI) and electrospray ionization (ESI), are commonly used in LC/MS. APCI and ESI are affinity methods in which the analytes either protonate or form adducts in the positive ion mode and deprotonate or attach electrons in the negative ion mode. These properties are generally associated with polar compounds. Common problems for ion molecular affinity ionization methods such as APCI and ESI are that the desired signal can be suppressed in APCI and ESI by compounds with higher charge affinities than the target compounds.

On the other hand, atmospheric pressure photoionization (APPI) is a new alternative ionization technique for LC/MS.[18–20,26] The APPI source is based on a high-frequency gas discharge lamp that generates vacuum-ultraviolet (VUV) photons of 10 and 10.6 eV energy. The energy of this discharge lamp is normally greater than the first ionization potential (IP) of the analyte because many organic compounds have IPs in the range of 7–10 eV. The IPs of the most commonly used solvents as mobile phase in LC also have higher IPs (water, IP = 12.6 eV; methanol, IP = 10.8 eV; acetonitrile, IP = 12.2 eV). Therefore, APPI may directly ionize only molecules of an analyte that has a relatively lower IP and may overcome the above-mentioned problem for APCI and ESI.

This paper focuses on the optimization and the suitability of LC/MS using the APPI technique for the determination of NIV and DON in wheat.

EXPERIMENTAL

Chemicals

The mycotoxins, NIV and DON, were purchased from Sigma Aldrich Japan (Tokyo, Japan). LC/MS grade methanol and reagent grade ammonium acetate were purchased from Wako Chemicals (Osaka, Japan). Pure water was purified with a Milli-Q system (Millipore, Tokyo, Japan). The cartridge column (MultiSep® #227; Romer Labs, Inc., Union, MO, USA) was purchased from Showa Denko Ltd. (Tokyo, Japan).

Liquid chromatography/mass spectrometry

An 1100 series LC system (Agilent Technologies, Waldbronn, Germany), consisting of a vacuum solvent degassing unit, a binary high-pressure gradient pump, an automatic sample injector and a column thermostat, was used for LC/MS analysis. A model 1100 series diode-array detector (Agilent Technologies, Waldbronn, Germany) was connected on-line with the mass-selective detector (MSD). LC separation was performed on a ZORBAX Eclipse XDB C18 column (150 mm × 2.1 mm i.d., 5 μm particle size; Agilent Technologies, Santa Clara, CA, USA) using a linear gradient from 90:10 A/B to 60:40 A/B in 20 min. Solvent A was water containing 10 mmol·L^{-1} ammonium acetate and solvent B was methanol. The flow rate was set at 0.2 mL·min^{-1} and the injection volume was 10 μL. Further, acetone was added after the diode-array detector at a flow rate of 60 μL·min^{-1} via a tee by an isocratic pump (Agilent Technologies, Waldbronn, Germany).

The MSD single quadrupole mass spectrometer was equipped with an orthogonal spray APPI source (Agilent Technologies, Santa Clara, CA, USA). Nitrogen used as nebulizer gas and drying gas in the ion source was generated from pressurized air by a AIR-TECHAT-10NP-CS nitrogen generator (Yokohama, Japan). For APPI, the nebulizer gas, the drying gas, the capillary voltage for the ion transmission, the fragmentor voltage for in-source fragmentation and the vaporizer temperature were set at 55 psi, 7 L·min^{-1}, 2500 V, 100 V and 300°C, respectively. The skimmer and entrance lens voltage in the ion source of the MSD were automatically optimized by a calibrant delivery system using a calibration standard (Agilent Technologies, Santa Clara, CA, USA) at 0.1 mL·min^{-1} and set to 27 V, 53 V. The LC/MS determination was performed by operating the MS system in the negative ion mode. Mass spectrum was acquired over a scan range *m/z* 100–500 using a step size of 0.1 Da and a scan speed of 0.5 scan·s^{-1}. Quantitative analysis was carried out using the selected ion monitoring (SIM) mode of a base ion peak at *m/z* 371 and 355 for NIV and DON, respectively, with a dwell time of 500 ms.

Sample preparation

The NIV and DON standard solutions at 100 μg·mL^{-1} for stock and fortification experiments were dissolved in acetonitrile, respectively. Then they were stored at 4°C in the dark until use. For preparation of a mixed working standard solution, an appropriate amount of individual stock standard was evaporated to dryness at 40°C under a gentle stream of nitrogen. The residue was dissolved in 1 mL of aqueous 10 mmol·L^{-1} ammonium acetate/methanol (90:10).

The domestic and imported wheat, totaling 56 samples, were obtained from a local retail store in Japan. For fortification experiments, 10 μL volumes of the NIV and DON mixture standard solutions at 100 and 10 μg·mL^{-1} were spiked to 10 g of blank wheat samples before extraction. Three replicates of two levels were prepared.

The extraction and clean-up for NIV and DON from samples were carried out as follows: 50 g of each sample were weighed in 500 mL Erlenmeyer flasks. After adding 200 mL acetonitrile/water (85:15), the flask was shaken for 60 min on an automatic shaker. The mixed solution was filtrated, and then 10 mL of the filtrate were applied to a MultiSep #227 cartridge column for the clean-up. The first 3 mL of eluate was discarded, but the next 2 mL were collected. They were evaporated to dryness at 40°C under a gentle stream of

DOI: 10.1002/rcm

nitrogen. The residue was dissolved in 0.5 mL aqueous 10 mmol·L^{-1} ammonium acetate/methanol (90:10).

RESULTS AND DISCUSSION

Optimization of the APPI parameters

To optimize the APPI conditions, different parameters which influence the ionization efficiency and a mass spectrum were investigated. The drying gas flow, the nebulizer gas pressure, the vaporizer temperature, the capillary voltage, the fragmentor voltage and the mobile phase were investigated under the chromatographic conditions mentioned in the Experimental section by using a acetate adduct ion (m/z = 371 and 355) as a target ion. However, the modification of the drying gas flow rate and the nebulizer gas pressure did not drastically improve the sensitivity of NIV and DON. Therefore, the effects of the fragmentor voltage, the capillary voltage, the vaporizer temperature and the mobile phase are described below.

APPI mass spectrum and effect of fragmentor voltage

There are three main means to produce an ion by APPI: (1) direct photoionization, (2) electron transfer with a dopant ion, or (3) proton transfer with a dopant or other protic gas-phase species. APPI makes use of a photoionizable dopant added to the vapor generated from the eluant to increase the ionization efficiency of the molecules in the vaporized LC eluant. Acetone or toluene is usually used as the dopant. In this study, acetone was added into the APPI source after the column at a flow rate of 60 μl·min^{-1}.

The fragmentor voltage is applied to the exit of the capillary and affects the transmission and fragmentation of sample ions between the exit of the capillary and the skimmer at relatively high pressure (3 Torr).[27,28] The fragmentor voltage helps the transfer of ions in the relatively high-pressure region between the exit of the capillary and the skimmer. In general, the higher the fragmentor voltage, the more fragment ions are produced. First of all, NIV and DON were ionized in positive ion mode. As a result, the $[M]^+$ radical cation (m/z 312) for NIV and $[M+H]^+$ protonated molecular ion (m/z 297) for DON were observed. However, many other fragment ions were observed and the intensities of $[M]^+$ and $[M+H]^+$ were very weak. Therefore, NIV and DON seem to have a higher ionization potential (IP) than 10.6 eV.

On the other hand, for the negative ion mode, the acetate adduct ion $[M+CH_3COO]^-$ was observed as the predominant ion for NIV and DON. In general, NIV and DON seem to have high volatile anion affinity because these compounds have more than three hydroxyl groups. Therefore, the ionization mechanism of APPI in the negative ion mode seems to experience an ion-molecular reaction with the acetate ion in the mobile phase, leading to the formation of the observed $[M+CH_3COO]^-$ ion. It is, however, beyond the scope of this article to expound on the ion-molecule chemistry of the APPI source. Thus, to establish the optimum fragmentor voltage for the analysis of NIV and DON in the negative ion mode, the intensity of this compound versus the fragmentor voltage was studied in the range from 80–200 V. As shown in Fig. 1, the optimum fragmentor voltage was found at 100 V, whereas a significant intensity reduction was observed at higher values. Further, the highest signal-to-noise (S/N) ratio was also observed at 100 V. The mass spectra of NIV and DON at the optimal voltage are shown in Fig. 2. These mass spectra showed that the $[M+CH_3COO]^-$ ion was the predominant ion. Based on the above results, the fragmentor voltage was set at 100 V.

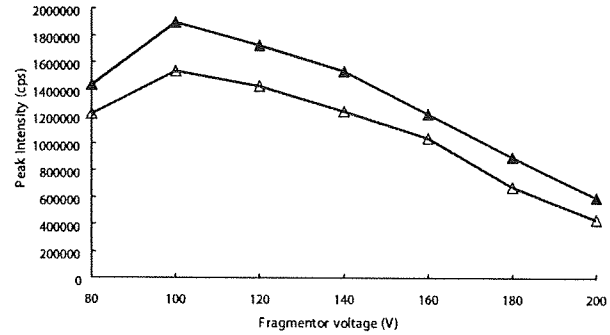

Figure 1. Effect of the fragmentor voltage on the peak intensities of NIV and DON. Concentration: 1 μg·mL^{-1}. For the other conditions, see Experimental section. ▲: NIV, Δ: DON.

Effect of capillary voltage

The capillary voltage is applied to the inlet of the capillary and influences the transmission efficiency of the ions through a capillary sampling orifice. There is one additional feature of the APPI source: ion formation by APPI does not require any element within the ionization region at a high potential unlike ESI and APCI, where the spray needle and corona discharge needle are operated at several kV. Therefore, the APPI source is essentially field-free. This characteristic allows for the independent optimization of the capillary voltage, which may have a tremendous effect on the sensitivity of the method. To establish the optimum capillary voltage, this parameter was varied from 1000 to 4000 V. As shown in Fig. 3, 1000 V was found to be optimum and a tremendous effect of this parameter on the intensity of NIV and DON was observed in the case where acetone was not used as the dopant. On the other hand, when acetone as the

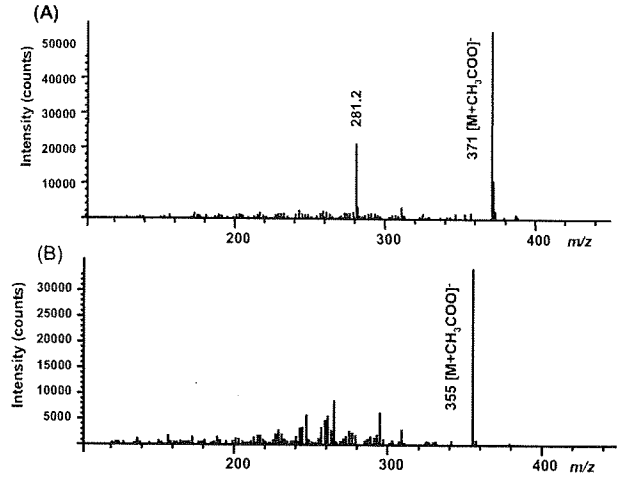

Figure 2. The mass spectra of (A) NIV and (B) DON.

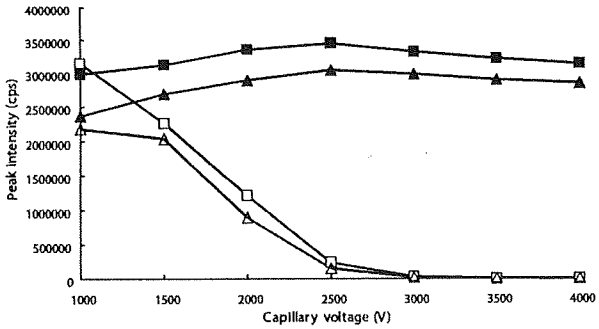

Figure 3. The effect of the capillary voltage on the peak intensity of NIV and DON. Concentration: 1 $\mu g \cdot mL^{-1}$. For the other conditions, see Experimental section. ■: NIV with acetone as dopant, ▲: DON with acetone as dopant, □: NIV without acetone, Δ: DON without acetone.

dopant was introduced into the APPI source, the maximum intensity of the ion was found at 2500 V and the intensity found at 2500 V with the dopant was a little higher than the maximum intensity at 1000 V without the dopant. The other important aspect is that the capillary voltage had an insignificant effect on the intensity by using the dopant and the ion current measured at the capillary inlet was much higher than it without the dopant. This result indicates that acetone as the dopant could generate enough electrons to improve the ionization efficiency and an excess amount of electrons could discount differences of the capillary voltage. Based on the above results, acetone was introduced into the APPI source and the capillary voltage was set at 2500 V.

Effect of vaporizer temperature

For APPI, the vaporizer temperature plays a key role for the complete evaporation of NIV and DON because ionization occurs in the vapor state like APCI. Thus, in the case of using linear gradient elution, this temperature must be kept high so that the change of mobile phase composition does not influence the ion intensity of NIV and DON. Under a high temperature, however, the risk of the thermal degradation occurs. In this study, the vaporizer temperature was varied between 250 and 400°C to optimize the intensity. The composition of the mobile phase was set at aqueous 10 $mmol \cdot L^{-1}$ ammonium acetate/methanol (90:10). As a result, the highest temperature for a maximum intensity of NIV and DON was at 300°C (data not shown). The intensity of NIV and DON decreased when the vaporizer temperature was set at 350°C and an intensive fragmentation was observed in the mass spectrum. Therefore, the decrease in the intensity over 350°C may be a result of the thermal degradation. Based on the above results, the vaporizer temperature was set at 300°C.

Effect of mobile phase

Generally speaking, APPI is a mass-flow-dependent ionization technique unlike ESI which is a concentration-dependent, because APPI occurs in the gas phase. However, Yang and Henion reported that for a neutral compound, an important observation with APPI is an apparent increase in sensitivity when the flow rate is reduced.[29] Then, the influence of the mobile phase flow rate on the intensity (the peak area) of NIV and DON in APPI was investigated by varying it from 0.2 to 1 $mL \cdot min^{-1}$. As a result, the maximum intensity of NIV and DON was found at 0.2 $mL \cdot min^{-1}$ and a drop in their intensity occurred beginning at flow rates higher than 0.2 $mL \cdot min^{-1}$. This result leads to the conclusion that the loss in the intensity of NIV and DON under high-flow conditions is mainly due to decreasing efficiency of the ionization process with increasing amount of eluent sprayed into the APPI source. On the basis of this result, the flow rate was set at 0.2 $mL \cdot min^{-1}$.

Linearity, detection limit and precision of the LC/APPI-MS system

At first, the analytical performance characteristics of the optimized LC/APPI-MS method were determined on standard solutions of NIV and DON in pure solvent. In order to achieve maximum sensitivity, all experiments were carried out in SIM mode using the mass corresponding to the $[M+CH_3COO]^-$ ions of NIV and DON. To test the linearity of the calibration curve, various concentrations of NIV and DON in the range from 0.2 to 100 $ng \cdot mL^{-1}$ were analyzed. As shown in Table 1, the repeatability of both methods for a standard solution was calculated on the basis of five replicates at 1 $ng \cdot mL^{-1}$ in the same day. The instrument detection limits (IDLs) were calculated as the peak-to-peak S/N ratio = 3 by using the mixture standard solution of NIV and DON (0.2 $ng \cdot mL^{-1}$). As shown in Table 1 and Fig. 4, IDLs and the relative standard deviations (RSDs) of NIV and DON

Table 1. Instrument detection limits and precision of NIV and DON in standard solution injected with 10 μL

Mycotoxin	Instrument detection limits[a] (pg)	Repeatability[b] (RSD, %)
NIV	0.8	1.9
DON	1.1	2.4

[a] Instrument detection limits defined as S/N ratio = 3.
[b] Repeatability was calculated on the basis of five replicates.

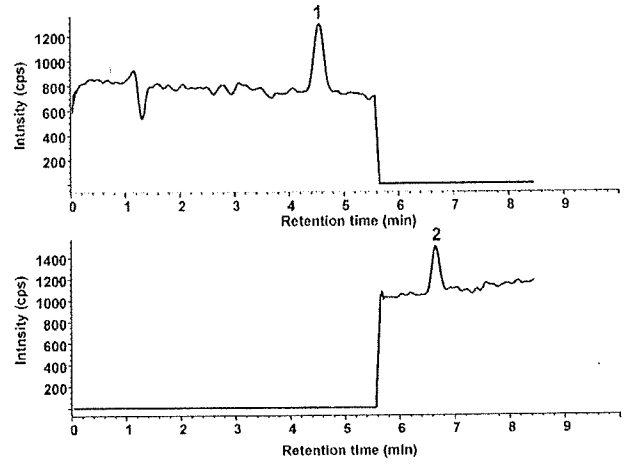

Figure 4. SIM chromatograms of NIV and DON in pure solvent at 0.2 $ng \cdot mL^{-1}$ with APPI. 1: NIV, 2: DON.

Table 2. Limits of detection and precision of the method for NIV and DON in wheat samples

Mycotoxin	Limits of detection[a] ($ng \cdot g^{-1}$)	Repeatability[b] (RSD, %)
NIV	0.20	2.9
DON	0.39	4.0

[a] Limits of detection defined as S/N ratio = 3.
[b] Repeatability was calculated on the basis of three replicates.

injected with 10 μL were 0.8 pg, 1.9% and 1.1 pg, 2.4%, respectively. Also, the limits of detection (LODs) of NIV and DON in wheat were determined by the signal corresponding to three times the background noise on each SIM chromatogram for the sample spiked at 10 $ng \cdot g^{-1}$. The LODs and RSDs of NIV and DON were 0.20 $ng \cdot g^{-1}$, 2.9% and 0.39 $ng \cdot g^{-1}$, 4.0%, respectively (Table 2).

Evaluation of APPI for the analysis of NIV and DON in wheat

In general, affinity-based ionization techniques, such as APCI and ESI, are susceptible to competition for charge effects due to some matrix components that coelute with analytes. Therefore, the matrix effect in the APPI determination was investigated by comparing the SIM chromatogram obtained from the standard solution in pure solvent with one obtained from a matrix-matched standard solution prepared from the analyte-free wheat extract. As can be seen from the data in Fig. 5, it was observed that the wheat matrix did not lead to significant alternations in the chromatograms. Furthermore, the RSDs of NIV and DON with APPI were 6.0% and 4.5%, respectively, which were calculated on the basis of five replicates at mixture standard solution with 20 $ng \cdot mL^{-1}$. Also, ionization was comparatively examined in APPI, ESI and APCI modes under the chromatographic conditions described in the Experimental section with SIM.

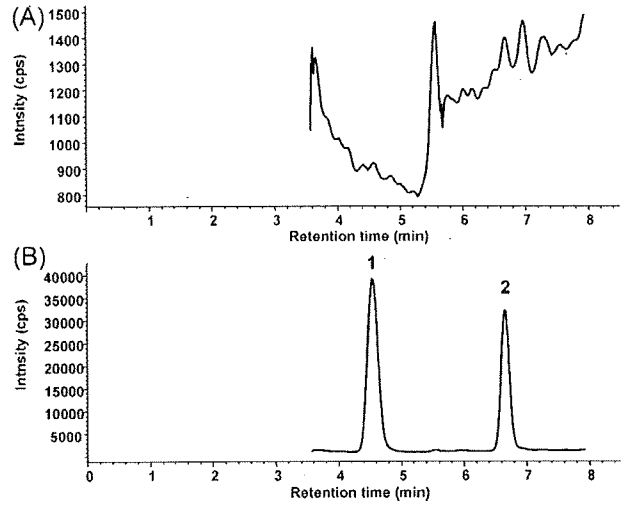

Figure 5. SIM chromatograms of (A) wheat extract and (B) a spiked wheat extract at 20 $ng \cdot g^{-1}$ NIV and DON. 1: NIV, 2: DON.

As a result, it was found that the APPI mode provided the optimum intensity for each mycotoxin. On the other hand, ESI mode created the highest matrix effect for each mycotoxin. In addition, the S/N ratios with APCI of NIV and DON were 80% and 30% lower than with APPI, respectively (data not shown). Thus, the APPI mode was selected to analyze NIV and DON throughout this study. These results indicate that APPI has the lower matrix effect. Then, a calibration curve in standard solutions was compared with one in wheat extract in the range from 0.2 to 100 $ng \cdot mL^{-1}$ by using APPI. As presented in Table 3, there is no significant difference in calibration equations and coefficient of determination. These results indicate that it is possible to use external standards instead of matrix-matched standards. This property of APPI is very useful for high-throughput applications because it minimizes the need to prepare matrix-matched standards.

To evaluate recoveries, the proposed method was applied to the analysis of spiked wheat samples of NIV and DON. Wheat samples were spiked at final concentrations of 100 $ng \cdot g^{-1}$ and 10 $ng \cdot g^{-1}$ for NIV and DON. The mean recoveries of each mycotoxin in wheat ranged from 86 to 107%, as shown in Table 4. At the same concentration, repeatability was performed (n = 3) indicating that the RSD ranged from 1.0 to 2.9% (Table 4).

Table 3. Linearity of calibration equation in a standard solution and wheat extract

		Calibration equation	r^{2a}
Standard solution	NIV	$y = 52323\ x + 1032$	0.9997
	DON	$y = 32467\ x + 932$	0.9997
Wheat extract	NIV	$y = 51378\ x + 1423$	0.9996
	DON	$y = 32848\ x + 1245$	0.9995

[a] r^2 is coefficient of determination.

Table 4. Recovery of NIV and DON in wheat

Mycotoxin	Concentration ($ng \cdot g^{-1}$)	Recovery[a] (%)	Repeatability[a] (RSD, %)
NIV	10	86	2.9
	100	86	1.0
DON	10	107	1.9
	100	100	1.1

[a] Recovery was calculated on the basis of three replicates.

Table 5. Natural occurrence of NIV and DON in wheat

Group	Analyzed No.	No. of samples: Positive (Incidence, %) NIV	DON	Mean ($ng \cdot g^{-1}$) NIV	DON	Range ($ng \cdot g^{-1}$) NIV	DON
Imported wheat	20	9 (45)	15 (75)	2	134	1–7	1–740
Domestic wheat	36	34 (94)	33 (92)	9	424	1–27	1–2248
Overall	56	43 (77)	48 (86)	7	333	1–27	1–2248

RCM

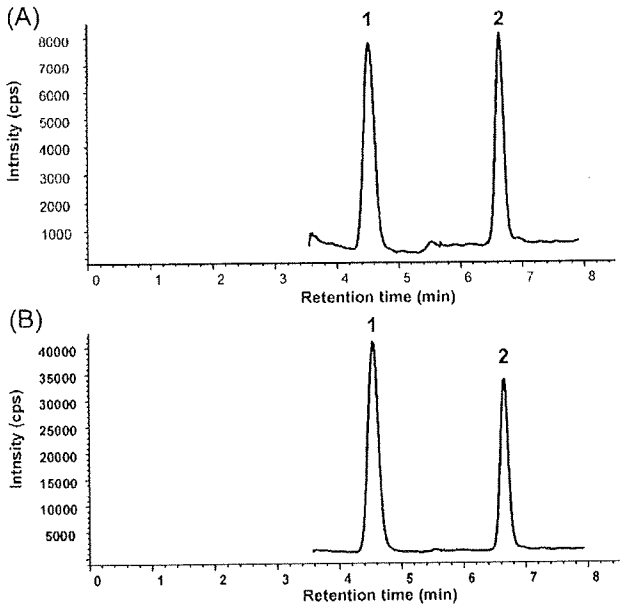

Figure 6. SIM chromatograms of naturally contaminated wheat samples. 1: NIV, 2: DON. Occurrence concentrations: (A) NIV, 4.8 ng·g^{-1}; DON, 5.8 ng·g^{-1} and (B) NIV, 21.2 ng·g^{-1}; DON, 20.9 ng·g^{-1}.

APPI method evaluation

To evaluate the proposed method, this method was applied to the analysis of 56 samples of wheat. The analytical results are summarized in Table 5 and a typical chromatogram from the wheat extract is shown in Fig. 6. NIV and DON were positive in 43 (77%) and 48 (86%) samples, respectively. Their average contents in the positive samples were estimated to be 7 (NIV) and 333 (DON) ng·g^{-1}. These data indicated that the proposed method is convenient for routine analysis of NIV and DON residues in wheat at high sensitivity levels.

CONCLUSIONS

In conclusion, APPI is an ideal ionization technique for high-sensitivity and high-selectivity analysis of NIV and DON in wheat. An important advantage of using APPI to determine the NIV and DON content of wheat is that matrix effect was not observed. Consequently, the proposed method eliminates the need for matrix-matched standards, which is more tedious for the samples from different origins. Further, validation data indicated that this method was convenient for routine analysis of NIV and DON residues in wheat at trace levels, since excellent recoveries and repeatability for samples were demonstrated.

REFERENCES

1. Yoshizawa T, Jin YZ. *Food Addit. Contam.* 1995; **12**: 689.
2. Kim JC, Kang HJ, Lee DH, Lee YW, Yoshizawa T. *Appl. Environ. Microbiol.* 1993; **59**: 3798.
3. Tanaka T, Yamamoto S, Hasegawa A, Aoki N, Besling JR, Sugiura Y, Ueno Y. *Mycopathologia* 1990; **110**: 19.
4. Schollenberger M, Muller HM, Rufle M, Suchy S, Plank S, Drochner W. *Mycopathologia* 2006; **161**: 43.
5. Rasmussen PH, Ghorbani F, Berg T. *Food Addit. Contam.* 2003; **20**: 396.
6. Ryu JC, Yang JS, Song YS, Kwon OS, Park J, Chang IM. *Food Addit. Contam.* 1996; **13**: 333.
7. Tanaka T, Hasegawa A, Matsuki Y, Ishii K, Ueno Y. *Food Addit. Contam.* 1985; **2**: 259.
8. Tanaka T, Hasegawa A, Yamamoto S, Lee U-S, Sugiura Y, Ueno Y. *J. Agric. Food Chem.* 1988; **36**: 979.
9. Lee U-S, Jang H-S, Tanaka T, Hasegawa A, Oh Y-J, Ueno Y. *Food Addit. Contam.* 1985; **2**: 185.
10. Ueno Y. *Trichothecenes – Chemical, Biological and Toxicological Aspects*, Ueno Y (ed.). Elsevier: Amsterdam, 1983; 135–146.
11. Takahashi M, Shibutani M, Sugita-Konishi Y, Aihara M, Inoue K, Woo G-H, Fujimoto H, Hirose M. *Food Chem. Toxicol.* 2008; **46**: 253.
12. WHO. *Safety Evaluation of Certain Mycotoxins in Food*, WHO Food Additives Series 47, World Health Organization: Geneva, 2001.
13. European Commission. *Opinion of the Scientific Committee on Food on Fusarium Toxins*, part 4.1, Nivalenol. SCF/CS/CNTM/MYC/26 Final, 2000.
14. Kostiainen R. *J. Chromatogr.* 1991; **562**: 555.
15. Kostiainen R, Kuronen P. *J. Chromatogr.* 1991; **543**: 39.
16. Tiebach R, Blaas W, Kellert M, Steinmeyer S, Weber R. *J. Chromatogr.* 1987; **318**: 103.
17. Razzazi-Fazeli E, Bohm J, Luf W. *J. Chromatogr. A* 1999; **854**: 45.
18. Robb DB, Covey TR, Bruins AP. *Anal. Chem.* 2000; **72**: 3653.
19. Syage JA, Evans MD, Hanold KA. *Am. Lab.* 2000; **32**: 24.
20. Rauha H, Vuorela H, Kostianen R. *J. Mass Spectrom.* 2001; **36**: 1269.
21. Tanaka T, Yoneda A, Inoue S, Sugiura Y, Ueno Y. *J. Chromatogr. A* 2000; **882**: 23.
22. Tiebach R, Blaas W, Kellert M, Steinmeyer S, Weber R. *J. Chromatogr.* 1985; **318**: 103.
23. Kostiainen R, Matsuura K, Nojima K. *J. Chromatogr.* 1991; **583**: 323.
24. Voyksner RD, Hagler WM, Swanson SP. *J. Chromatogr.* 1987; **394**: 183.
25. Rajkyla E, Lassasenaho K, Sakkers P. *J. Chromatogr.* 1987; **384**: 391.
26. Kertesz V, Van Berkel G. *J. Am. Soc. Mass Spectrom.* 2002; **13**: 109.
27. Takino M, Daishima S, Yamaguchi K. *Anal. Sci.* 2000; **16**: 70.
28. Takino M, Daishiman S, Yamaguchi K, T. Nakahara T. *J. Chromatogr. A* 2001; **928**: 53.
29. Yang C, Henion J. *J. Chromatogr. A* 2002; **970**: 155.

Toxicology Letters 192 (2010) 150–154

Contents lists available at ScienceDirect

Toxicology Letters

journal homepage: www.elsevier.com/locate/toxlet

Deoxynivalenol and nivalenol inhibit lipopolysaccharide-induced nitric oxide production by mouse macrophage cells

Kei-ichi Sugiyama[a,*], Masashi Muroi[b], Ken-ichi Tanamoto[b], Motohiro Nishijima[c], Yoshiko Sugita-Konishi[a]

[a] Division of Microbiology, National Institute of Health Sciences, 1-18-1 Kamiyoga, Setagaya-ku, Tokyo 158-8501, Japan
[b] Research Institute of Pharmaceutical Sciences, Musashino University, 1-1-20 Shinmachi, Nishitokyo-shi, Tokyo 202-8585, Japan
[c] Department of Food and Health Science, Jissen Women's University, 4-1-1 Osakaue, Hino, Tokyo 191-8510, Japan

ARTICLE INFO

Article history:
Received 26 June 2009
Received in revised form 15 October 2009
Accepted 15 October 2009
Available online 24 October 2009

Keywords:
Lipopolysaccharide
Inducible nitric oxide synthase
Macrophage
Deoxynivalenol
Nivalenol

ABSTRACT

Deoxynivalenol (DON) and nivalenol (NIV), trichothecene mycotoxins, are secondary metabolites produced by *Fusarium* fungi. Trichothecene mycotoxins cause immune dysfunction, thus leading to diverse responses to infection. The present study evaluated the effect of DON and NIV on nitric oxide (NO) production by RAW264 cells stimulated with lipopolysaccharide (LPS). LPS-induced NO production was reduced in the presence of these toxins. The transcriptional activation and expression of inducible NO synthase (iNOS) by LPS were also repressed by these toxins. DON or NIV inhibited LPS-induced expression of interferon-β (IFN-β), which plays an indispensable role in LPS-induced iNOS expression. These results indicate that DON and NIV inhibit the LPS-induced NO and IFN-β production, which both play an important role for host protection against invading pathogens, and suggests that the inhibition of these factors may be involved in the immunotoxic effects of these mycotoxins.

1. Introduction

Deoxynivalenol (DON), one of the trichothecene mycotoxins, is a secondary metabolite produced by *Fusarium* fungi and a contaminant found in wheat, barley and corn worldwide (Rotter et al., 1996). In addition, nivalenol (NIV), which belongs to the type B trichothecenes, and DON are also detected in cereals harvested in Japan, Korea and other limited areas (Lee et al., 2002). Trichothecene mycotoxins have been implicated in vomiting and alimentary hemorrhage (Bennett and Klich, 2003). Moreover, many studies have previously shown that immune cells such as B and T cells, NK cells and macrophages are sensitive to DON (Instanes and Hetland, 2004; Pestka, 2008), and trichothecene mycotoxins including DON induce dysregulation of the immune response (Pestka and Smolinski, 2005; Sugita-Konishi and Pestka, 2001) and is able to either enhance or suppress resistance to pathogens such as *Salmonella* (Tai and Pestka, 1990; Ziprin and Elissalde, 1990) and reovirus (Li et al., 2007). The immunotoxic effects of DON reduce resistance against *Listeria monocytogenes* infection (Tryphonas et al., 1986).

Nitric oxide (NO) plays an important role in the protection against intracellular microbiostasis, with organisms such as *L. monocytogenes*, *Chlamydophila pneumoniae* and protozoa (Boockvar et al., 1994; Sakai et al., 2006). *Mycobacterium tuberculosis*, which can infect and replicate in macrophages, inhibits the recruitment of inducible NO synthase (iNOS) to mycobacterial phagosomes (Miller et al., 2004). NO production by specific stimuli-activated macrophage is regulated by iNOS, which is a Ca^{2+}-independent enzyme. The expression of iNOS is dramatically induced by lipopolysaccharide (LPS), which is a component of the Gram-negative bacteria cell wall, in murine macrophages (Shimomura-Shimizu et al., 2005). iNOS expression by activated macrophages depends on several transcriptional factors, including activator protein 1, signal transducer and activator of transcription-1 (STAT-1) and interferon regulatory factor-1 (IRF-1) (Sakai et al., 2006). Furthermore, interferon-β (IFN-β) signaling in an autocrine/paracrine fashion is indispensable for LPS-induced iNOS expression (Shimomura-Shimizu et al., 2005). LPS-induced IFN-β expression causes activation of STAT and IRF proteins and iNOS expression, which induces NO production in murine macrophages stimulated with LPS (Jacobs and Ignarro, 2001). IFN-β also plays an important role in protecting the host from viral infections (Haller et al., 2006).

This study examined the effect of DON and NIV on NO production by activated macrophages to understand the novel immunotoxicity of these mycotoxins. DON and NIV caused the

* Corresponding author. Tel.: +81 3 3700 1141; fax: +81 3 3700 9852.
E-mail address: sugiyama@nihs.go.jp (K.-i. Sugiyama).

0378-4274/$ – see front matter © 2009 Elsevier Ireland Ltd. All rights reserved.
doi:10.1016/j.toxlet.2009.10.020

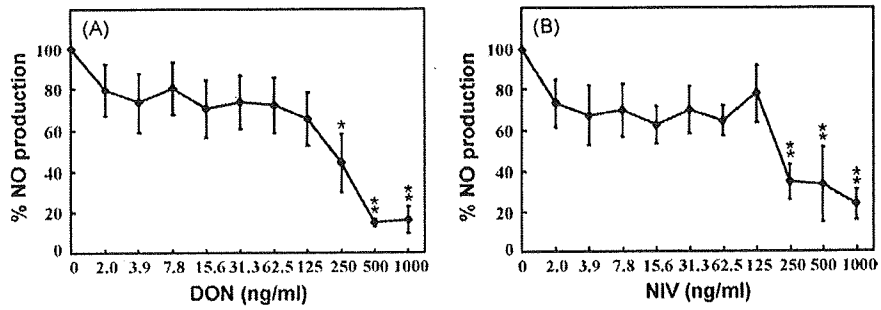

Fig. 1. Concentration-dependent effects of DON and NIV on LPS-induced NO production by RAW264 cells. RAW264 cells were stimulated with LPS (10 ng/ml) in the presence of the indicated concentrations of DON (A) or NIV (B) for 24 h. The culture supernatants were analyzed for NO levels. NO induced by LPS treatment alone is expressed as 100%. Values are presented as the means ± SEM from three or four independent experiments. Statistical analysis was performed using one-way ANOVA followed by Dunnett's post hoc test (*$P < .05$; **$P < .01$, vs control).

inhibition of LPS-induced NO production, in which the decrease in iNOS expression might be partly caused by the reduction of IFN-β production.

2. Materials and methods

2.1. Cell culture and reagents

A mouse macrophage cell line RAW264 (obtained from the Riken Cell Bank, Tsukuba, Japan) was cultured in DMEM (Gibco-BRL, Rockville, MD) supplemented with 10% (vol/vol) heat-inactivated fetal calf serum (Gibco-BRL), penicillin (100 U/ml) and streptomycin (100 μg/ml). DON and NIV were bought from Wako Purechemical Industries, Ltd. (Osaka, Japan) and biopure Referenzsubstanzen GmbH (Tulln, Austria), respectively. LPS from *Escherichia coli* O111:B4 was purchased from Sigma–Aldrich (St. Louis, MO). Anti-rabbit iNOS antibody (M-19) and anti-goat actin antibody (C-11) were purchased from Santa Cruz Biotechnology, Inc. (Santa Cruz, CA). Horseradish peroxidase conjugated anti-mouse and goat secondary antibodies were obtained from Jackson ImmunoResearch (West Grove, PA).

2.2. NO production

RAW264 cells were plated ($1–5 \times 10^5$ cells/well) in 96-well plates and on the following day stimulated for 24 h. NO production was determined by measuring the concentration of nitrite in culture supernatants with Griess reagent (Shimomura-Shimizu et al., 2005).

2.3. Western blot analysis

Cellular extracts were prepared as described (Shimomura-Shimizu et al., 2005). The same amount of protein, determined by the Bradford method, was loaded onto each lane of a discontinuous SDS–10% polyacrylamide gel (acrylamide/bisacrylamide ratio, 29:1) and then electrophoresis was performed according to the method of Laemmli (Laemmli, 1970). Proteins transferred to a polyvinylidene difluoride membrane (Immobilon-P; Millipore Corp., Bedford, MA) were subjected to Western blotting with either rabbit anti-iNOS (1:1000) or goat anti-Actin (1:1000) as the primary antibodies and subsequently detected with peroxidase conjugated species-specific IgG (1:10,000). The signals were visualized using an enhanced chemiluminescence system (Amersham Biosciences, Piscataway, NJ).

2.4. Reporter assay

The iNOS reporter assay was performed as previously described (Shimomura-Shimizu et al., 2005). RAW264 cells ($3–5 \times 10^5$ cells/well) were plated in 12-well plates before transfection. The cells were transfected on the following day using FuGeneHD (Roche Diagnostics GmbH Mannheim, Germany) with 1 μg of pGmiNF which possess mouse iNOS promoter region fused with firefly luciferase gene. At 24 h following transfection, cells were stimulated for 6 h, and the reporter gene activity was measured by Dual-LuciferaseTM Reporter Assay System (Promega, Madison, WI) according to the manufacturer's instructions. Luciferase activities were normalized by protein concentration.

The IFN-β reporter assay were performed using RAW264 which were stably transfected with IFN-β reporter plasmid consisting of the mouse IFN-β promoter region fused with the firefly luciferase gene (Ohnishi et al., 2008). The reporter activity driven by the IFN-β promoter was measured as described above.

2.5. Statistical analysis

Statistical comparison of multiple groups was analyzed using one-way ANOVA followed by Dunnett's post hoc test. The values are expressed as the mean ± SEM.

3. Results

3.1. Effects of DON and NIV on LPS-induced NO production

DON and other trichothecenes dysregulate the immune system *in vitro* (Pestka and Smolinski, 2005; Sugita-Konishi and Pestka, 2001). In addition, NO production by activated macrophages is affected by trichothecenes. LPS-induced NO production by a mouse macrophage cell line RAW264 in the presence of DON or NIV was measured to examine the effects of DON and NIV on NO release from activated macrophages. RAW264 cells were treated with LPS and each trichothecene for 24 h, and then the culture supernatants were assessed for NO. DON suppressed LPS-induced NO production by RAW264 cells in a concentration-dependent manner, and a high significant inhibitory effect was observed at concentrations as low as 500 ng/ml (Fig. 1A). Similar results were obtained when LPS-induced NO production by RAW264 cells was measured in the presence of NIV (Fig. 1B).

3.2. Effects of DON and NIV on LPS-induced iNOS expression

NO production by macrophages in response to specific stimuli is catalyzed by iNOS protein. Therefore, to investigate the mechanism of the inhibitory effect of DON and NIV on LPS-induced NO production, iNOS protein expression was examined by Western blotting in RAW264 cells. LPS treatment significantly induced the expression of iNOS protein and both trichothecenes suppressed the iNOS expression in a dose-dependent manner. On the other hand, the protein levels of actin were not affected by both trichothecenes, suggesting that DON and NIV did not induce cellular toxicity up to 1000 ng/ml (Fig. 2).

The induction of iNOS protein in macrophages is mainly regulated at the transcriptional level (Jacobs and Ignarro, 2001; Lowenstein et al., 1993; Xie et al., 1993). The iNOS promoter activity was evaluated using a mouse iNOS promoter-luciferase construct. When the cells were treated with 500–1000 ng/ml of DON, the LPS-induced reporter activity was significantly inhibited (Fig. 3A). NIV at 125–1000 ng/ml also significantly repressed the LPS-induced reporter activity (Fig. 3B).

3.3. Effects of DON and NIV on LPS-induced IFN-β expression

The autocrine/paracrine signaling of IFN-β, which is released in response to LPS, plays an important role in the induction of

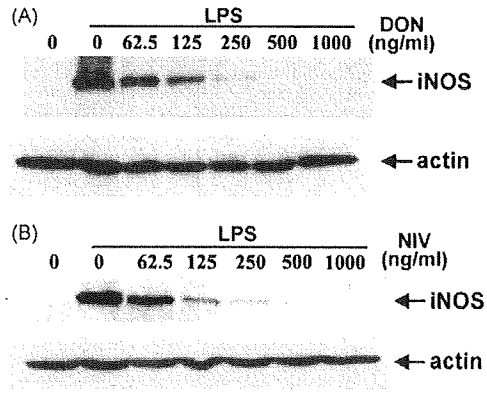

Fig. 2. Effects of DON and NIV on LPS-induced iNOS expression. RAW264 cells were stimulated with LPS (10 ng/ml) for 6 h with or without the indicated concentrations of DON (A) or NIV (B). The cell lysates were prepared and analyzed for iNOS and actin proteins by Western blotting. The results are representative of three independent experiments.

iNOS protein in mouse macrophages (Jacobs and Ignarro, 2001). To further investigate the mechanisms by which DON and NIV suppressed LPS-induced NO production, the effect of these toxins on LPS-induced IFN-β promoter activity was evaluated. The IFN-β reporter activity was significantly induced by LPS, and more than 250 ng/ml of DON and NIV significantly reduced the reporter activity, although the LPS-induced reporter activity was not completely inhibited, even at 1000 ng/ml (Fig. 4).

4. Discussion

LPS-induced NO production by RAW264 cells was dose-dependently inhibited by DON and NIV. These toxins also suppressed LPS-induced iNOS promoter activity and expression of iNOS protein in a similar concentration range to that of the inhibition effect on NO production, indicating that transcriptional inhibition is involved in the repression of LPS-induced NO production.

This study also revealed that the LPS-induced IFN-β reporter activity was repressed by these toxins. IFN-β plays an important role in iNOS expression (Jacobs and Ignarro, 2001; Thomas et al., 2006). It is also reported to induce upregulation of iNOS transcription (Zheng et al., 2006). In the current study, DON and NIV inhibited, although not completely, LPS-induced IFN-β production by RAW264 cells. Therefore, these results suggest that the decrease in IFN-β production is, at least partly, involved in the inhibition of iNOS expression. Toll-like receptor 4 (TLR4) transmits LPS-recognition signals to stimulate IFN-β production via the Toll/IL-1 receptor domain-containing adaptor inducing IFN-β (TRIF)-dependent pathway (Yamamoto et al., 2002). There-

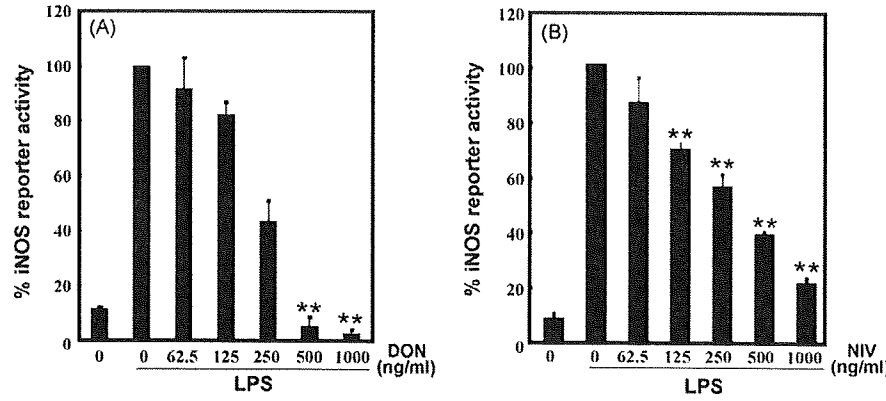

Fig. 3. Effects of DON and NIV on LPS-induced iNOS reporter activity. RAW264 cells were transiently transfected with a mouse iNOS reporter plasmid. After 24 h, cells were stimulated with LPS (10 ng/ml) for 6 h with or without the indicated concentrations of DON (A) or NIV (B) and luciferase activity was then measured. The reporter activity in response to LPS alone is expressed as 100%. Values are the means ± SEM from three independent experiments. Statistical analysis was performed using one-way ANOVA followed by Dunnett's post hoc test (**$P < .01$ vs LPS treated control).

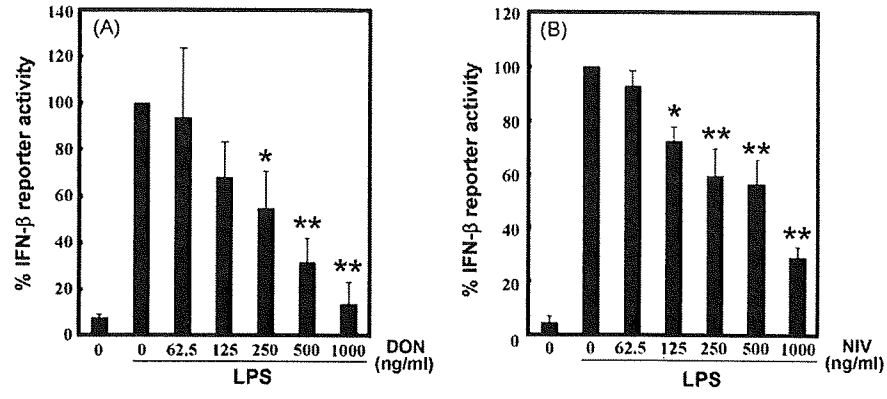

Fig. 4. Effects of DON and NIV on LPS-induced IFN-β reporter activity. RAW264 cells stably transfected with an IFN-β reporter plasmid were stimulated with LPS (10 ng/ml) for 6 h with or without the indicated concentrations of DON (A) or NIV (B) and luciferase activity was then measured. The reporter activity in response to LPS alone is expressed as 100%. Values are the means ± SEM from three independent experiments. Statistical analysis was performed using one-way ANOVA followed by Dunnett's post hoc test (*$P < .05$; **$P < .01$, vs LPS treated control).

fore, DON or NIV might suppress the TRIF-dependent pathway of TLR4 signaling, leading to the inhibition of NO production from macrophages stimulated with LPS. Further studies are required to clarify the effect of DON and NIV on the TLR4 signaling pathway.

Previous studies have demonstrated that trichothecenes are able to cause immune dysfunction through dysregulated production of pro-inflammatory mediators by leucocytes (Pestka and Smolinski, 2005; Sugita-Konishi and Pestka, 2001). DON-induced expression of pro-inflammatory mediators including interleukin-6 (IL-6), IL-1β and tumor necrosis factor-α are induced at transcriptional and translational levels, in which activated mitogen-activated protein kinases including p38 are involved (Amuzie et al., 2008; Bae and Pestka, 2008; Pestka and Amuzie, 2008). In addition, the expression of DON-induced pro-inflammatory cytokine is upregulated in the presence of LPS in human and mouse macrophages (Sugita-Konishi and Pestka, 2001; Zhou et al., 1999). However, the present results show that the induction of iNOS expression associated with p38 activation (Choi et al., 2008) was reduced by DON or NIV. A transcriptional factor, IRF-1, which binds to the IFN-β gene regulatory elements and promotes transcriptional activation of the IFN-β gene, is also important for induction of iNOS (Bachmaier et al., 1997; Kimura et al., 1994; Miyamoto et al., 1988; Rodel et al., 1999; Shao et al., 2007). Therefore, it is possible that the reduction of LPS-induced iNOS expression in the presence of DON or NIV may be primarily mediated by IRF-1.

NO contributes to the host defense against infections with intracellular bacteria including those that can be considered re-emerging pathogens such as *M. tuberculosis* and *L. monocytogenes* (Boockvar et al., 1994; El Kasmi et al., 2008). Therefore, future research should focus on the isolation of the TLR4 signaling molecules modulated by DON and NIV, which frequently contaminate grains including wheat, would be of particular importance.In summary, DON and NIV suppressed LPS-induced NO and IFN-β production, which both play an important role for host protection against invading pathogens. These results may provide insight into the dysregulation of the immune response induced by trichothecenes.

Conflict of interest

There are no conflicts of interest.

Acknowledgements

This work was supported by a Health and Labor Sciences Research Grant from the Ministry of Health, Labor and Welfare of Japan. The authors gratefully acknowledge Dr. Yoichi Kamata and Dr. Hodaka Suzuki for valuable discussions of the manuscript. The authors are also grateful to Hiroko Furusawa for her excellent technical assistance.

References

Amuzie, C.J., Harkema, J.R., Pestka, J.J., 2008. Tissue distribution and proinflammatory cytokine induction by the trichothecene deoxynivalenol in the mouse: comparison of nasal vs. oral exposure. Toxicology 248, 39–44.

Bachmaier, K., Neu, N., Pummerer, C., Duncan, G.S., Mak, T.W., Matsuyama, T., Penninger, J.M., 1997. iNOS expression and nitrotyrosine formation in the myocardium in response to inflammation is controlled by the interferon regulatory transcription factor 1. Circulation 96, 585–591.

Bae, H.K., Pestka, J.J., 2008. Deoxynivalenol induces p38 interaction with the ribosome in monocytes and macrophages. Toxicol. Sci. 105, 59–66.

Bennett, J.W., Klich, M., 2003. Mycotoxins. Clin. Microbiol. Rev. 16, 497–516.

Boockvar, K.S., Granger, D.L., Poston, R.M., Maybodi, M., Washington, M.K., Hibbs Jr., J.B., Kurlander, R.L., 1994. Nitric oxide produced during murine listeriosis is protective. Infect. Immun. 62, 1089–1100.

Choi, H.J., Eun, J.S., Park, Y.R., Kim, D.K., Li, R., Moon, W.S., Park, J.M., Kim, H.S., Cho, N.P., Cho, S.D., Soh, Y., 2008. Ikarisoside A inhibits inducible nitric oxide synthase in lipopolysaccharide-stimulated RAW 264.7 cells via p38 kinase and nuclear factor-kappaB signaling pathways. Eur. J. Pharmacol. 601, 171–178.

El Kasmi, K.C., Qualls, J.E., Pesce, J.T., Smith, A.M., Thompson, R.W., Henao-Tamayo, M., Basaraba, R.J., Konig, T., Schleicher, U., Koo, M.S., Kaplan, G., Fitzgerald, K.A., Tuomanen, E.I., Orme, I.M., Kanneganti, T.D., Bogdan, C., Wynn, T.A., Murray, P.J., 2008. Toll-like receptor-induced arginase 1 in macrophages thwarts effective immunity against intracellular pathogens. Nat. Immunol. 9, 1399–1406.

Haller, O., Kochs, G., Weber, F., 2006. The interferon response circuit: induction and suppression by pathogenic viruses. Virology 344, 119–130.

Instanes, C., Hetland, G., 2004. Deoxynivalenol (DON) is toxic to human colonic, lung and monocytic cell lines, but does not increase the IgE response in a mouse model for allergy. Toxicology 204, 13–21.

Jacobs, A.T., Ignarro, L.J., 2001. Lipopolysaccharide-induced expression of interferon-beta mediates the timing of inducible nitric-oxide synthase induction in RAW 264.7 macrophages. J. Biol. Chem. 276, 47950–47957.

Kimura, T., Nakayama, K., Penninger, J., Kitagawa, M., Harada, H., Matsuyama, T., Tanaka, N., Kamijo, R., Vilcek, J., Mak, T.W., et al., 1994. Involvement of the IRF-1 transcription factor in antiviral responses to interferons. Science 264, 1921–1924.

Laemmli, U.K., 1970. Cleavage of structural proteins during the assembly of the head of bacteriophage T4. Nature 227, 680–685.

Lee, T., Han, Y.K., Kim, K.H., Yun, S.H., Lee, Y.W., 2002. Tri13 and Tri7 determine deoxynivalenol- and nivalenol-producing chemotypes of *Gibberella zeae*. Appl. Environ. Microbiol. 68, 2148–2154.

Li, M., Harkema, J.R., Cuff, C.F., Pestka, J.J., 2007. Deoxynivalenol exacerbates viral bronchopneumonia induced by respiratory reovirus infection. Toxicol. Sci. 95, 412–426.

Lowenstein, C.J., Alley, E.W., Raval, P., Snowman, A.M., Snyder, S.H., Russell, S.W., Murphy, W.J., 1993. Macrophage nitric oxide synthase gene: two upstream regions mediate induction by interferon gamma and lipopolysaccharide. Proc. Natl. Acad. Sci. U.S.A. 90, 9730–9734.

Miller, B.H., Fratti, R.A., Poschet, J.F., Timmins, G.S., Master, S.S., Burgos, M., Marletta, M.A., Deretic, V., 2004. Mycobacteria inhibit nitric oxide synthase recruitment to phagosomes during macrophage infection. Infect. Immun. 72, 2872–2878.

Miyamoto, M., Fujita, T., Kimura, Y., Maruyama, M., Harada, H., Sudo, Y., Miyata, T., Taniguchi, T., 1988. Regulated expression of a gene encoding a nuclear factor, IRF-1, that specifically binds to IFN-beta gene regulatory elements. Cell 54, 903–913.

Ohnishi, T., Yoshida, T., Igarashi, A., Muroi, M., Tanamoto, K., 2008. Effects of possible endocrine disruptors on MyD88-independent TLR4 signaling. FEMS Immunol. Med. Microbiol. 52, 293–295.

Pestka, J.J., 2008. Mechanisms of deoxynivalenol-induced gene expression and apoptosis. Food Addit. Contam., 1–13.

Pestka, J.J., Amuzie, C.J., 2008. Tissue distribution and proinflammatory cytokine gene expression following acute oral exposure to deoxynivalenol: comparison of weanling and adult mice. Food Chem. Toxicol. 46, 2826–2831.

Pestka, J.J., Smolinski, A.T., 2005. Deoxynivalenol: toxicology and potential effects on humans. J. Toxicol. Environ. Health B: Crit. Rev. 8, 39–69.

Rodel, J., Groh, A., Hartmann, M., Schmidt, K.H., Lehmann, M., Lungershausen, W., Straube, E., 1999. Expression of interferon regulatory factors and indoleamine 2,3-dioxygenase in *Chlamydia trachomatis*-infected synovial fibroblasts. Med. Microbiol. Immunol. 187, 205–212.

Rotter, B.A., Prelusky, D.B., Pestka, J.J., 1996. Toxicology of deoxynivalenol (vomitoxin). J. Toxicol. Environ. Health 48, 1–34.

Sakai, K., Suzuki, H., Oda, H., Akaike, T., Azuma, Y., Murakami, T., Sugi, K., Ito, T., Ichinose, H., Koyasu, S., Shirai, M., 2006. Phosphoinositide 3-kinase in nitric oxide synthesis in macrophage: critical dimerization of inducible nitric-oxide synthase. J. Biol. Chem. 281, 17736–17742.

Shao, L., Guo, Z., Geller, D.A., 2007. Transcriptional suppression of cytokine-induced iNOS gene expression by IL-13 through IRF-1/ISRE signaling. Biochem. Biophys. Res. Commun. 362, 582–586.

Shimomura-Shimizu, M., Sugiyama, K., Muroi, M., Tanamoto, K., 2005. Alachlor and carbaryl suppress lipopolysaccharide-induced iNOS expression by differentially inhibiting NF-kappaB activation. Biochem. Biophys. Res. Commun. 332, 793–799.

Sugita-Konishi, Y., Pestka, J.J., 2001. Differential upregulation of TNF-alpha, IL-6, and IL-8 production by deoxynivalenol (vomitoxin) and other 8-ketotrichothecenes in a human macrophage model. J. Toxicol. Environ. Health A 64, 619–636.

Tai, J.H., Pestka, J.J., 1990. T-2 toxin impairment of murine response to *Salmonella typhimurium*: a histopathologic assessment. Mycopathologia 109, 149–155.

Thomas, K.E., Galligan, C.L., Newman, R.D., Fish, E.N., Vogel, S.N., 2006. Contribution of interferon-beta to the murine macrophage response to the toll-like receptor 4 agonist, lipopolysaccharide. J. Biol. Chem. 281, 31119–31130.

Tryphonas, H., Iverson, F., So, Y., Nera, E.A., McGuire, P.F., O'Grady, L., Clayson, D.B., Scott, P.M., 1986. Effects of deoxynivalenol (vomitoxin) on the humoral and cellular immunity of mice. Toxicol. Lett. 30, 137–150.

Xie, Q.W., Whisnant, R., Nathan, C., 1993. Promoter of the mouse gene encoding calcium-independent nitric oxide synthase confers inducibility by interferon gamma and bacterial lipopolysaccharide. J. Exp. Med. 177, 1779–1784.

Yamamoto, M., Sato, S., Mori, K., Hoshino, K., Takeuchi, O., Takeda, K., Akira, S., 2002. Cutting edge: a novel Toll/IL-1 receptor domain-containing adapter that pref-

erentially activates the IFN-beta promoter in the Toll-like receptor signaling. J. Immunol. 169, 6668–6672.
Zheng, H., Yu, X., Collin-Osdoby, P., Osdoby, P., 2006. RANKL stimulates inducible nitric-oxide synthase expression and nitric oxide production in developing osteoclasts. An autocrine negative feedback mechanism triggered by RANKL-induced interferon-beta via NF-kappaB that restrains osteoclastogenesis and bone resorption. J. Biol. Chem. 281, 15809–15820.
Zhou, H.R., Harkema, J.R., Yan, D., Pestka, J.J., 1999. Amplified proinflammatory cytokine expression and toxicity in mice coexposed to lipopolysaccharide and the trichothecene vomitoxin (deoxynivalenol). J. Toxicol. Environ. Health A 57, 115–136.
Ziprin, R.L., Elissalde, M.H., 1990. Effect of T-2 toxin on resistance to systemic *Salmonella typhimurium* infection of newly hatched chickens. Am. J. Vet. Res. 51, 1869–1872.